

Bergslagen etapp 1

Geophysical and geochemical characterisation of graphite-bearing rocks in the Giltjärn– Skrammelfall area northwest of Norberg

Peter Hedin & Torbjörn Bergman

september 2020

SGU-rapport 2020:26



Cover: Remains of historical mining equipment used for extraction of graphite ore from the Skrammelfall mine, Norberg.
Photo: Torbjörn Bergman

Authors: Peter Hedin and Torbjörn Bergman
Reviewed by: Mehrdad Bastani and Benno Kathol
Head of unit: Ildikó Antal Lundin
Editor: Lina Rönnåsen
Geological Survey of Sweden
Box 670, 751 28 Uppsala
phone: 018-17 90 00
e-mail: sgu@sgu.se
www.sgu.se

CONTENT

Abstract.....	4
Sammanfattning.....	4
Introduction	5
Regional geology.....	6
Regional geophysics	8
Airborne geophysics.....	8
Gravity.....	10
Geological field observations and sampling.....	12
The Skrammelfall mines in the area west of Lake Stora Alten	12
The Giltjärn mines.....	14
Ekorrsvedsgruvan.....	16
The Styggberget area	17
Petrophysical properties	18
Geophysical survey, results and discussion	20
Conclusions.....	24
References	25
Appendix A. Lithochemical analysis results.....	26
Methods.....	26
Appendix B. Petrophysical analysis results.....	33

ABSTRACT

As part of an assignment appointed by the Ministry of Enterprise and Innovation that focuses on critical raw material in Sweden, survey activities were carried out in several locations in the Bergslagen region (Claeson et al. 2020). The present report presents a more detailed summary of the investigations and analyses carried out in one of the key areas of interest northwest of Norberg, Västmanland county in 2019. This key area also falls within the framework of the SGU-project Bergslagen, etapp 1 and SGU's mineral resources inventory of Västmanland county (Bergman et al. in prep).

The investigated area has been chosen to be of specific interest due to past mining of graphite – one of the minerals that the European commission and the Swedish government has classified as innovation critical. The area includes known graphite occurrences at Lake Norra Gilltjärnen, the Skrammelfall mines near Lake Stora Alten and the trial pit Ekorrsvedsgruvan further northeast.

Magnetometric and very low frequency electromagnetic (VLF) measurements were performed along nine profiles. Geological field observations, litho-geochemical and petrophysical analyses of rock samples collected from outcrop and mining waste piles are used to support the analysis of the geophysical profile data.

The chemical analyses of mining waste from the Skrammelfall mines show graphite-bound carbon contents up to 32% in gneissic metasedimentary rock belonging to the Larsbo formation. Results from the present investigation show that the electrically conductive graphite bearing rock may continue to depths of about 50 m at the Skrammelfall mines and down to 100 m depth at the Gilltjärnen mines. In addition, geophysical data also indicate a continuation of the Skrammelfall graphite bearing rocks under Lake Norra Gilltjärnen, an area that has never been mined or investigated by e.g. drilling.

SAMMANFATTNING

Inom det av näringsdepartementet angivna regeringsuppdraget “Uppdrag att kartlägga innovationskritiska metaller och mineral” (diarienummer: N2018/01044/FÖF) som tidigare rapporterats av Claeson m.fl. (2020), utfördes undersökningar vid flera platser inom Bergslagen. Denna rapport ger en mer detaljerad sammanfattning av de undersökningar och analyser som utfördes 2019 i ett område nordväst om Norberg, Västmanlands län. Studien faller också inom ramen för SGUs projekt Bergslagen, etapp 1 samt SGUs mineralresursinventering av Västmanlands län (Bergman m.fl., under arbete).

Området valdes ut som speciellt intressant på grund av historisk brytning av grafit – ett av de mineral som både europeiska kommissionen och svenska regeringen benämnt som innovationskritiska. Undersökningsområdet inkluderar kända fyndigheter vid Norra Gilltjärnen, Skrammelfallsgruvorna nära Stora Alten och en provbrytning Ekorrsvedsgruvan längre åt nordost.

Magnetometri och lågfrekventa elektromagnetiska (Very Low Frequency, VLF) mätningar utfördes längs nio profiler och kompletterades med geologiska observationer samt litogeokemiska och petrofysiska analyser av insamlat bergartsmaterial från berghällar och varphögar.

Kemisk analys av varpmaterial från Skrammelfallsgruvorna visar ett innehåll av grafitbundet kol på upp till 32 % i gnejsig metasedimentär bergart tillhörande Larsboformationen. Resultat från föreliggande undersökning, från inversion av elektromagnetiska data, visar att den elektriskt ledande grafitförande bergarten kan fortsätta till cirka 50 m djup vid Skrammelfallsgruvorna och ner till 100 m djup vid Gilltjärnsgruvorna. Dessutom indikerar geofysiska data att den grafitförande bergarten vid Skrammelfallsgruvorna kan ha en fortsättning under sjön Norra Gilltjärnen, vilken tidigare aldrig varit föremål för gruvbrytning eller närmare undersökning genom till exempel borrhög.

INTRODUCTION

The Giltjärn–Skrammelfall area northwest of Norberg in Västmanland county hosts several known graphite occurrences of which some have been mined in the past, i.e. the Giltjärn and Skrammelfall mines northwest of Halvarsbenning (fig. 1). Aside from the Giltjärn and Skrammelfall mines a minor mining attempt, *Ekorrsvedsgruvan*, is known from the area. The graphite occurrences are distributed over a distance of c. 7 km in a northeast–southwest oriented line. The mineralisations are hosted by a metasedimentary rock sequence generally referred to as the Larsbo series (Lundqvist & Hjelmqvist 1937, Hjelmqvist 1938) later called Larsbo formation by Strömberg (1983, fig. 1).

The graphite mineralisations are known since the beginning of the 19th century and were mined to some extent towards the end of the 1800's (Lindroth 1918). Mining continued in the beginning of 1900's and the most important mining period was during the years 1914–1917 when approximately 3000 tons of graphite ore were extracted from the Skrammelfall mines (Tegengren 1924). The deepest mine in the area, mined down to at least 20 m depth, is the *Gamla Skrammelfallsgruvan*. However, most of the mines and trial pits in the area are less than 5 m deep.

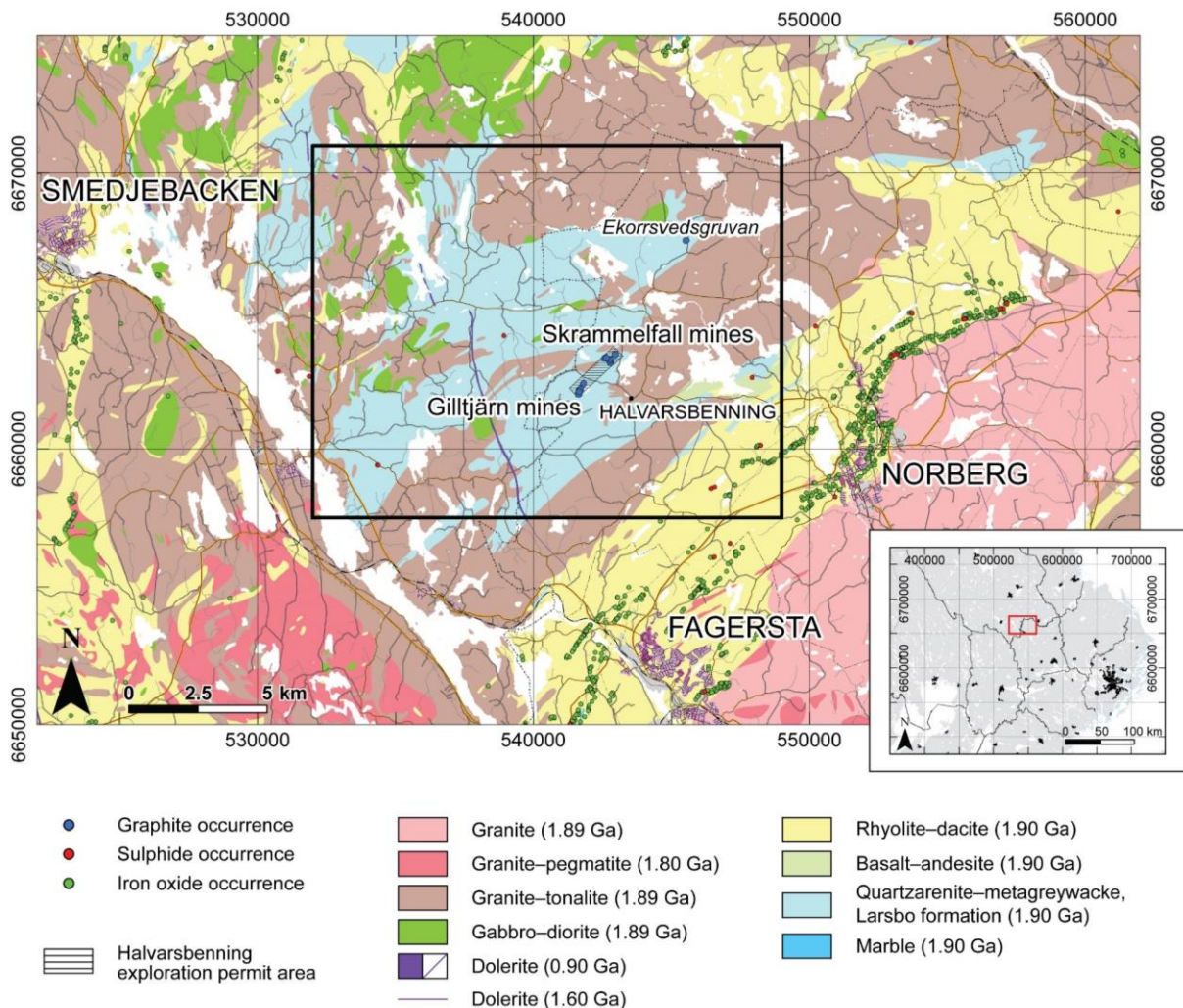


Figure 1. Simplified bedrock geological map over the Norberg-Fagersta area based on SGU's digital bedrock database (Berggrund 1:50 000–250 000). The black rectangle shows the location of Figures 2–5.

The area is also of interest for current exploration. Asera Mining AB was recently granted an exploration permit (named Halvarsbänning), by the Mining Inspectorate of Sweden (Bergsstaten), which allows graphite exploration in the area encompassing the old abandoned graphite mines at Giltjärn and Skrammelfall (fig. 1).

The aim of the present survey is to increase the knowledge about the graphite bearing rocks and mineralisations in the area and to evaluate their geographical distribution and geological context. A graphite bearing horizon in the bedrock is typically a good electrical conductor. Graphite is generally associated with pyrrhotite, which also is a good electrical conductor and additionally has strong magnetic properties. Information about the depth extent and regional continuation of graphite bearing horizons can therefore be evaluated using modern geophysical techniques; both directly with the VLF method, which is sensitive to electrical conductors, and indirectly with magnetometry which is sensitive to variation in magnetic properties within the bedrock.

To investigate a potential extension at depth and a regional continuation of the known graphite occurrences, combined magnetometric and VLF measurements were conducted along nine surface profiles in three focus areas (fig. 2). The geophysical ground measurements were supported by geological field observations of outcrops as well as petrophysical, lithochemical and mineralogical analyses of rock samples from outcrops and waste rock dumps. This report presents the main results of these investigations.

REGIONAL GEOLOGY

The investigated area is situated in the central part of the Bergslagen mining district (Stephens & Jansson 2020, Stephens et al. 2009). The bedrock is dominated by approximately 1.9 Ga old metasedimentary rocks and metagranitoids (fig. 1). The simplified bedrock geological maps presented in figures 1 and 2 are based on SGU's digital bedrock database (Berggrund 1:50 000–1:250 000), which in the investigated area is based on SGU's bedrock maps in the scale of 1:50 000 (Strömberg 1983, Ambros 1986a, Ambros 1986b, Strömberg 1996).

The graphite mineralisations are generally hosted by fine-grained, relatively well-preserved silt-sandstones to argillites, locally with well-developed bedding (light blue in figures 1 and 2). These rocks have generally been interpreted as metagreywackes formed as turbidites, based on the occurrence of graded bedding noted in many places (Stephens et al. 2009).

The metasedimentary rock unit in the investigated area (light blue in figure 2) is generally referred to as the "Larsbo series" or "Larsbo formation" (Lundqvist & Hjelmqvist 1937, Hjelmqvist 1938, Strömberg 1983). The age and the stratigraphic level of these rocks have been subject for discussion for a long time (Törnebohm 1875, Mogensen 1934, Geijer 1936, Strömberg 1983, Ambros 1986, Stephens 2009). Geijer (1936) assumed the Larsbo formation to be younger than the felsic metavolcanic rocks hosting the iron ores in the Norberg-Fagersta area (1.9 Ga). However, later mapping in the area indicated that the Larsbo formation in fact is older than the felsic metavolcanic rocks (Strömberg 1983, Ambros 1986, Stephens 2009). U–Pb dating of detrital zircons from a quartzite in the area has yielded zircon ages in the range 2.04 to 1.90 Ga as well as 2.97 to 2.60 Ga (Claesson et al. 1993). These data imply that the quartzite was deposited prior to 1.90 Ga and relatively close in time to the volcanic activity (Stephens et al. 2009).

The present investigation is focused on the mineralisations and their host rocks with respect to their geophysical, geochemical and mineralogical character and has not dealt with the stratigraphic issue of the Larsbo formation.

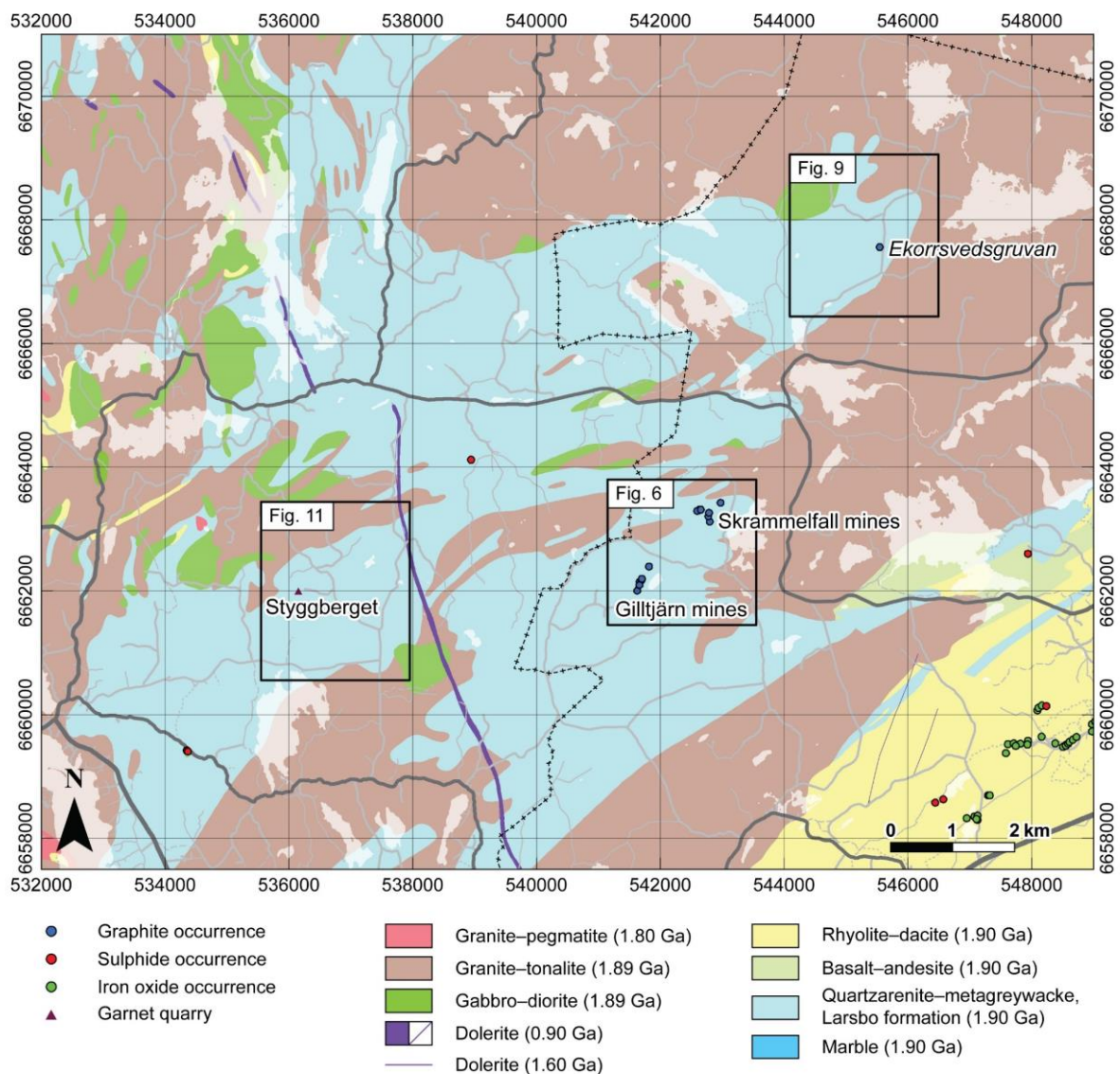


Figure 2. Bedrock geological map over the Giltjärn-Skrammelfall area and surroundings based on SGU's digital bedrock database (Berggrund 1:50 000–250 000). The black rectangles show the three focus areas of the present investigation.

REGIONAL GEOPHYSICS

Airborne geophysics

During 2016, SGU conducted an airborne geophysical survey over the region where the geomagnetic field intensity, the electromagnetic data, namely very low frequency (VLF), and natural gamma radiation were measured. The current acquisition systems are composed of a Scintrex CS 2 magnetometer with <0.3 nT precision, a Radiation Solutions RSX 5 spectrometer, and an SGU built dual-frequency VLF instrument with sampling intervals of c. 7 m, 16 m, and 16 m, respectively. The survey was flown at 60 m nominal altitude and 200 m line separation, with lines oriented at 130° azimuth (clockwise from north) to be favourable for modelling and interpretation of the regional mineralised formations in the Norberg and Ludvika areas, which have a predominantly SW to NE orientation. This flight direction is also favourable for mapping and modelling of the mineralisation in the Giltjärn and Skrammelfall mining areas.

Intrusive rocks generally give rise to a fairly homogenous anomaly pattern due to relatively homogenous distribution of magnetic minerals (with higher magnetic susceptibility) in the rock. Supracrustal rocks on the other hand, show a greater variation in the magnetic susceptibility, especially if they are hosting skarn and magnetite iron mineralisations or pyrrhotite sulphide mineralisations. Thus, supracrustal rocks and especially volcanic rocks, normally give rise to banded magnetic anomalies with a pattern that reflects the local variations in lithology and tectonic deformation.

Figure 3 shows the aeromagnetic anomaly map, whereas figure 4 shows the variation in electrical resistivity based on airborne VLF data. The latter is reciprocal to electrical conductivity, i.e. low resistivity anomalies means high electrical conductivity. The regional aeromagnetic and VLF data show that the Giltjärn and Skrammelfall mines lie in an anomalous band of both elevated magnetic field intensity (fig. 3) and low electrical resistivity (fig. 4). The magnetic anomalies at the Giltjärn and Skrammelfall mines have a similar signature but are separated and may be two parallel horizons or a repetition of the same horizon in a fold structure. Another similarly strong anomaly is seen c. 100 m east of the Giltjärn mines, beneath Lake Norra Giltjärnen and surrounding wetlands. Therefore, this may represent a pyrrhotite and graphite bearing horizon which is parallel with that hosting the Giltjärn mines and possibly a continuation of the Skrammelfall mineralisation.

The geophysical maps based on the airborne data (figures 3 and 4), show several areas within the metasedimentary rocks of the Larsbo formation, with similar strong and coincident anomalies in the magnetic field intensity and electrical resistivity. This may indicate elevated pyrrhotite concentrations and possibly the occurrence of occasionally associated graphite bearing rock. The known graphite occurrence at *Ekorrsvedsgruvan*, located c. 5 km northeast of the Giltjärn and Skrammelfall mines, is situated in areas with distinct anomalies on both magnetic and resistivity maps (figures 3 and 4). Similar anomalies are also seen to the west and northwest of the Giltjärn and Skrammelfall mines (figures 3 and 4), suggesting additional areas where the bedrock potentially contains significant amounts of pyrrhotite and graphite.

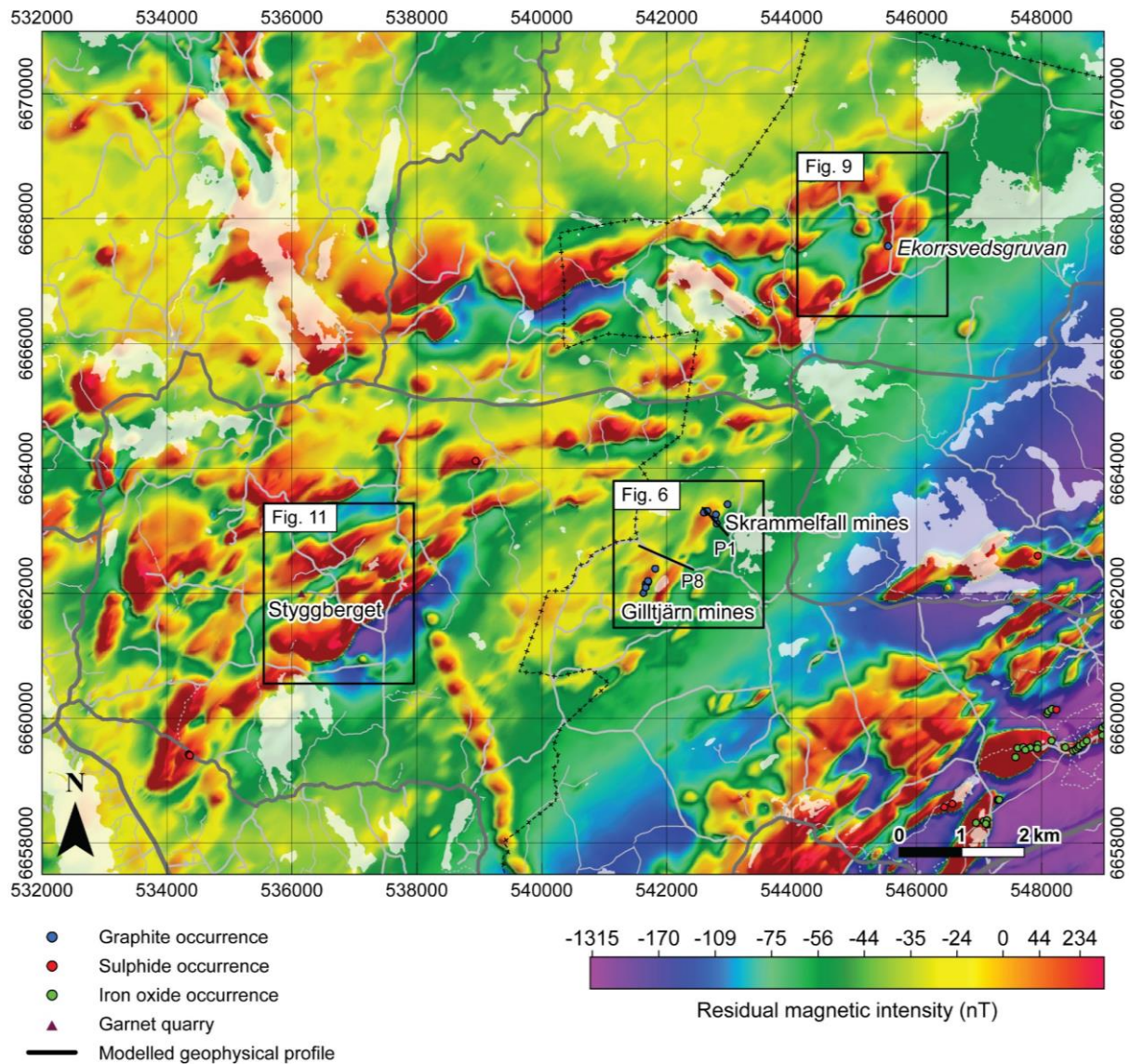


Figure 3. Residual magnetic field anomaly based on aeromagnetic measurements from 2016, calculated as the difference between the measured total magnetic field intensity after reduction to pole and the 1 km upward continuation of the same. Positive anomalies (red colours) typically indicate the presence of ferro- and ferrimagnetic minerals among which magnetite and pyrrhotite are known from the area. All known graphite occurrences are seen to lie along magnetic anomalies which are caused by the high pyrrhotite concentrations in the graphite bearing rock. The strong positive anomalies in the southeast are primarily caused by magnetite iron ore which is dominant in the Norberg area. Results from surface-based magnetometry along profile P1 and P8 (black lines) are shown together with airborne measurements and results from inversion of ground VLF data in figures 13 and 14. The black rectangles show the three focus areas of the present investigation.

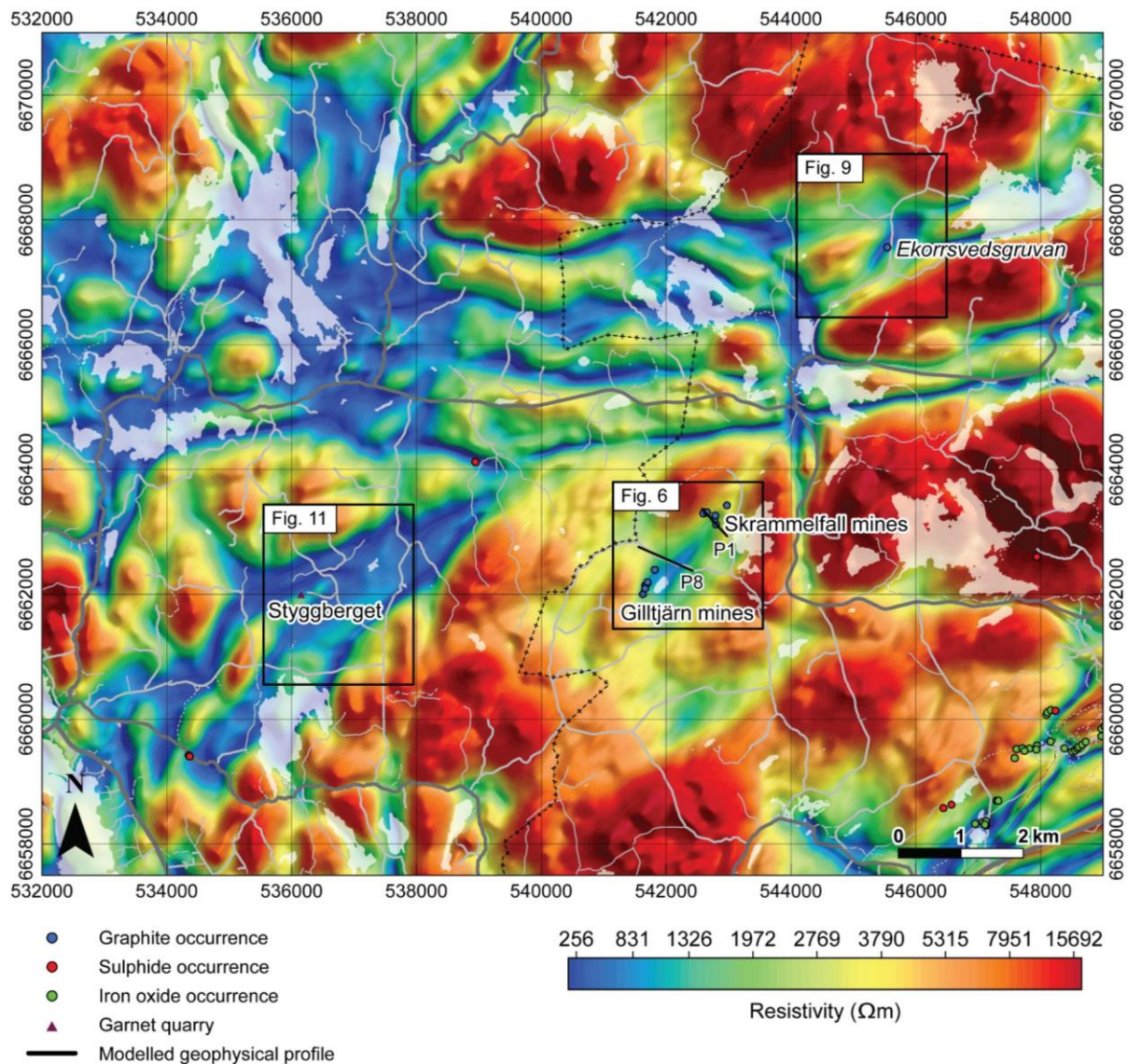


Figure 4. Apparent resistivity calculated from airborne VLF measurements acquired in 2016. Low resistivity anomalies (blue colours) represent areas of high electrical conductivity that may be generated by mineralised zones or water-bearing faults and fracture systems or possibly caused by infrastructures such as powerlines and railroads. The low resistivity anomaly that connects the Gilltjärn and Skrammelfall mining areas coincide with a positive magnetic anomaly (compare with figure 3) and likely reflect the geographical distribution of the known mineralisations. Negative resistivity anomalies are also seen to correlate with strong magnetic anomalies in e.g. the Ekorrsvedsgruvan and Styggberget area. Results from 2D inversion of surface-based VLF-measurements along profile P1 and P8 (black lines) are shown in figures 13 and 14. The black rectangles show the three focus areas of the present investigation.

Gravity

Gravity data has previously been acquired in the area to achieve a regional data coverage with a distance between measurement locations of c. 1–1.5 km in average. Figure 5 shows the residual gravity anomaly, based on all available gravity data in the area and calculated as the difference between the terrain corrected Bouguer anomaly data and a 3 km upward continuation of the same.

In general, mafic bedrock formations or major mineralised zones have relatively high densities and give rise to positive gravity anomalies, whereas felsic bedrock in contrast has lower densities and generates negative gravity anomalies. A large positive gravity anomaly is observed in the

Styggerget area and two smaller in the Giltjärn-Skrammelfall and *Ekorrsvedsgruvan* areas. The gravity point distribution is not dense enough to resolve near-surface formations, however, these gravity highs correlate well with areas of positive anomalies in both magnetic intensity and electrical conductivity. The mass excess could thus be related to the elevated concentrations of the iron-sulphide pyrrhotite. In the Styggerget area, hosting the largest gravity anomaly, mafic intrusives are known from bedrock geological maps (fig. 2) directly to the northwest and to the southeast of the Styggerget focus area. A major mafic intrusion at depth below the area is thus also a potential cause of the geophysical response.

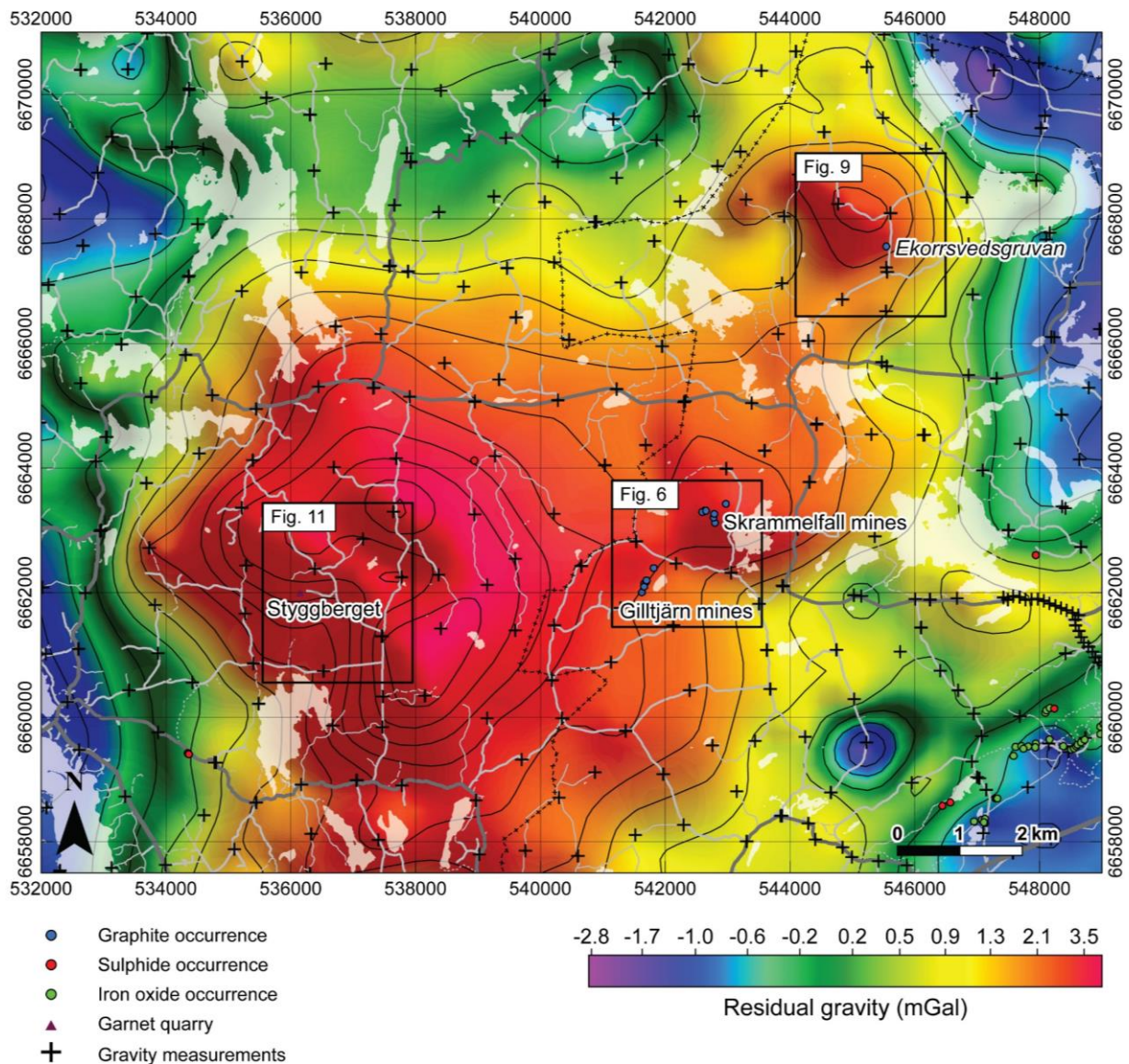


Figure 5. Residual gravity anomaly map based on gravity data acquired before 2019, calculated as the difference between the Bouguer anomaly and a 3 km upward continuation of the same. Contour lines represent isolines in the residual gravity anomaly drawn at 0.5 mGal interval. In general, mafic bedrock formations or major mineralised zones give rise to positive gravity anomalies while felsic bedrock generates negative gravity anomalies. Positive gravity anomalies correlate with some of the strongest anomalies in the airborne magnetic and VLF data (compare with figures 3 and 4). The black rectangles show the three focus areas of the present investigation.

GEOLOGICAL FIELD OBSERVATIONS AND SAMPLING

The following description of the graphite occurrences in the Norberg area is mainly based on field work in the area done in conjunction with the regional inventory of mineral resources in Västmanland county 2018 (Bergman et al. in prep).

Additional outcrop mapping, sampling and analyses were done during 2019. In total, 42 samples were collected for petrophysical analysis at SGU, see separate section below. The investigation also included litho-geochemical analyses of 17 samples from waste rock piles and outcrops adjacent to the known graphite occurrences, in order to define the chemical characteristics of the mineralisations and the concentrations of carbon tied to graphite. The complete analytical results, including carbon (C) and sulphur (S) of special interest, are presented in *Appendix A. Litho-geochemical analysis results*. Seven polished thin sections were prepared from samples of the graphite richest occurrences to determine in which form and mineralogical context graphite appears.

The Skrammelfall mines in the area west of Lake Stora Alten

Gamla Skrammelfallsgruvan is the largest mine in the area west of Lake Stora Alten and comprises four water-filled open pit mines in a row covering a distance of sixty meters (fig. 6). The graphite-bearing horizon is striking northeast–southwest and is, according to Tegengren (1924), 3–6 m wide and steeply dipping to the northwest.

The mine shafts vary between 10–15 m in length and are 4–6 m wide (fig. 7a). The water depth is at its deepest 20 m. Northeast of the mine there is a large pile of coarse waste rock consisting of a rust-weathered quartz-feldspar-muscovite-biotite gneiss with varying contents of graphite, pyrrhotite and pyrite (fig. 7b). Small amounts of chalcopyrite can also be noted. The magnetic susceptibility of the rock is relatively low and varies between $30\text{--}100 \times 10^{-5}$ SI.

Microscope examination of polished thin sections from waste rock samples, shows that the graphite is amorphous, fine-grained (0.01–0.1 mm) and usually occurs in bands, 1–5 cm thick.

Pyrrhotite is most common among the sulphide minerals. However, small amounts of pyrite, sphalerite and chalcopyrite are also noted, generally enclosed in pyrrhotite. Chalcopyrite also occurs as dissolution droplets in sphalerite.

Litho-geochemical analysis of samples from the waste rock shows that the carbon content varies between 22 and 30% (Appendix A). Older analyses reported even higher carbon content, up to 39% (Lindroth 1918). Copper and zinc levels are relatively low and vary between 204–453 ppm Cu and 166–925 ppm Zn (Appendix A).

In the area northeast and southeast of *Gamla Skrammelfallsgruvan* there are also some minor graphite occurrences, including *Haggrensgruvan*, *Blyertsgruvan* and *Kungsgruvan* (fig. 6). These are probably the mines described by Tegengren (1924) as the Altfall mines. No further information is found about their mineralogy or mining history. The following descriptions are based on observations made in conjunction with field visits in the area 2018 and 2019.

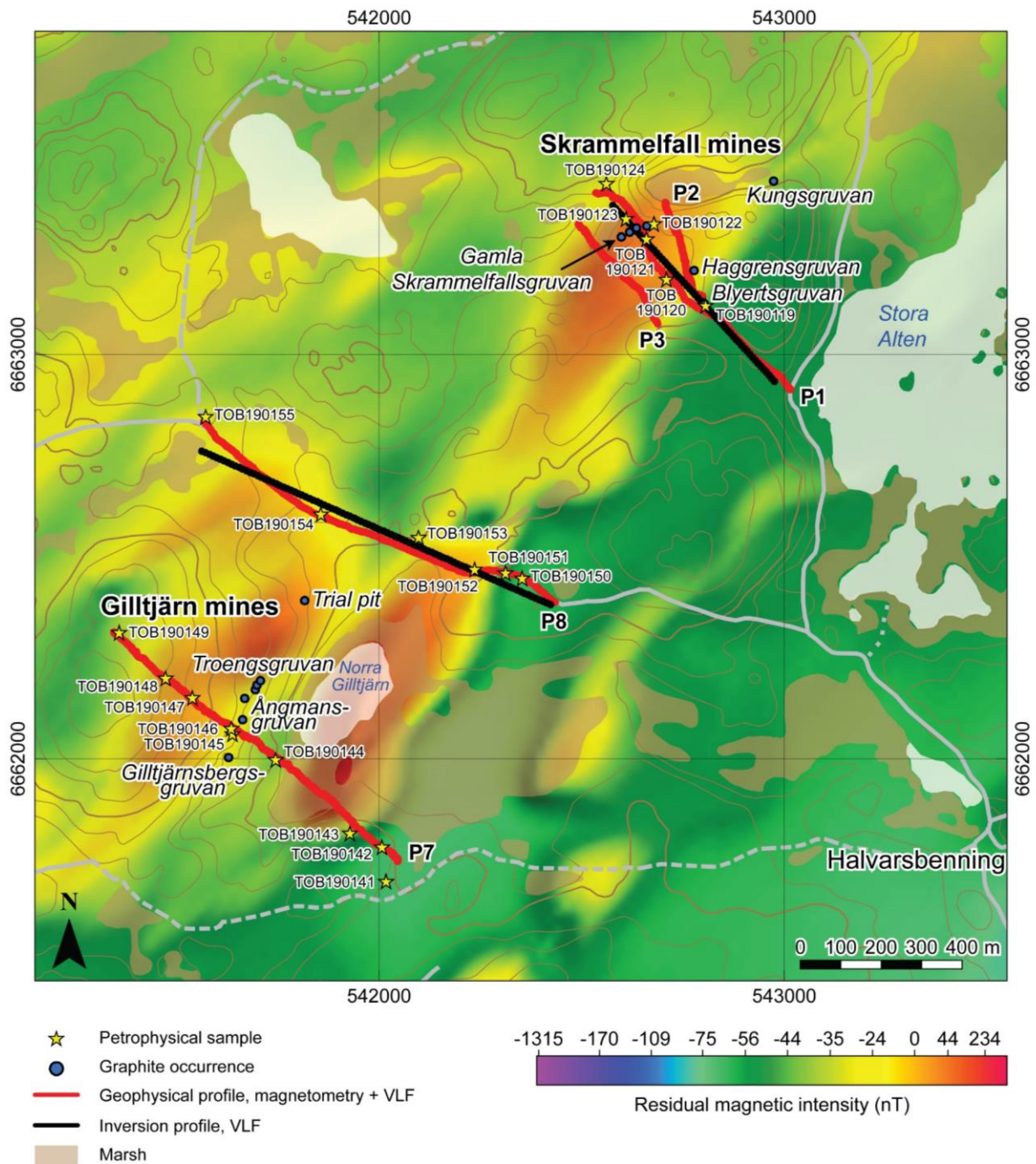


Figure 6. Residual magnetic field (see figure 3) in the Giltjärn–Skrammelfall area. Pyrrhotite is known from the Giltjärn and Skrammelfall mining areas, occurring together with the graphite. The anomaly suggests a link between the two mining areas, but also that the graphite bearing rock at the Skrammelfall mines may continue beneath Lake Norra Giltjärnen and surrounding wetlands. Magnetic and VLF measurements as well as 2D inversion of ground based VLF data along profile P1 and P8 (black line) are shown in figures 13 and 14.

Haggrensgruvan (6663207-542777), situated 150 m southeast of *Gamla Skrammelfallsgruvan*, is a timber-lined, water-filled shaft, 3×2 m wide and 7 m deep (fig. 7c). A pile of waste rock is found 15 m south of the pit and consist of fine-grained metagreywacke with small amounts of pyrrhotite, pyrite and graphite. Chemical analysis of a rock sample from the waste rock dump only shows a carbon content of 0.23 % (Appendix A).



Figure 7. (a) Gamla Skrammelfallsgruvan. (b) Graphite-rich metagreywacke from the waste rock dump at Gamla Skrammelfallsgruvan. (c) The Haggrensgruvan mine shaft. (d) Graphite rich metasedimentary rock from the Blyertsgruvan. Photos: Torbjörn Bergman.

Blyertsgruvan (6663125-542803), situated 240 m south east of *Gamla Skrammelfallsgruvan*, is a water-filled pit, 4 m deep, 4×4 m wide. Adjacent to the pit there is a pile of waste rock consisting of fine-grained mica-rich metasedimentary rock with only small amounts of pyrrhotite and graphite. However, some pieces are dark grey and relatively rich in graphite (fig. 7d). Chemical analyses show that the graphite rich rock type contains 32% C, whereas the fine-grained metasedimentary rock contains less than 0.23% C (Appendix A).

Kungsgruvan (6663125-542803), situated 330 m northeast of *Gamla Skrammelfallsgruvan*, consists of two trial pits next to each other on a northeast–southwest striking line. Both pits are less than 2 m deep and the northeastern pit is 3×6 m wide while the southwestern one is 4×4 m. Adjacent to the holes there is a small heavily overgrown pile of waste rock with fine-grained, grey, rusty mica-rich metasedimentary rocks with small amounts of pyrrhotite, pyrite and graphite. No chemical analysis was made, but the carbon content is most likely less than 1%.

The Giltjärn mines

The Giltjärn mines are a row of small graphite mines and trial pits west of Lake Norra Giltjärnen approximately 1,500 m southwest of the Skrammelfall mines. The Giltjärn mines comprise three old mining concessions: *Troengsgruvan*, *Ångmansgruvan* and *Giltjärnsbergsgruvan* (see figure 6).

Troengsgruvan (6662171-541694), comprises three small, water-filled mines or trial pits in a row over a distance of sixty meters in northeast–southwestern direction (fig. 6). The water-filled pits are 3–4 m deep and 5–8 m across. Small amounts of waste rock are found adjacent to the pits and consist of fine-grained quartz and mica-rich metasedimentary rock with small amounts of pyrrhotite and graphite. A lithochemical analysis of a rock sample shows a carbon content of 0.18% (Appendix A). Furthermore, 250 m northeast of the three pits, there is an additional trial pit and a small exploration trench. The trial pit is 7×2 m and 1 to 2 m deep. The waste rock found adjacent to the pit consists of fine-grained metasedimentary rock without visible amounts of graphite or sulphide minerals. The exploration trench occurs 30 m southwest of the pit, it is a 20 m long in northwest–southeastern direction, perpendicular to the strike of the rock. The trench is 1 m wide and 1 m deep and is lacking visible outcrop or waste rock.

Ångmansgruvan (6662149-541668), comprises two small trial pits and a trench in the area southwest of *Troengsgruvan*. The largest trial pit, at given coordinate, is 10×10 m and 2 m deep (fig. 8). A few meters to the south there is an additional trial pit, 8×6 m and 2 m deep. Adjacent to the larger pit, there is a waste rock dump with the same type of fine-grained quartz-rich metasedimentary rock as that found at *Troengsgruvan*. However, some rock pieces in the dump, consist of dark grey graphite rich gneissic rock. A lithochemical analysis of this type shows a carbon content of 20,3% and 1.3% sulphur (Appendix A).

The trench is situated 50 m further to the south, and in the exposed rock side in the trench, both graphite bearing gneissic rock and fine-grained quartz-mica rich metasedimentary rock are exposed.

Gilltjärnsbergsgruvan, (6662004-541628), is the south-westernmost and largest of the mines west of Norra Gilltjärnen. The mine is water-filled, 20×15 m wide and 15 m deep. Only scattered pieces of waste rock are found adjacent to the mine but the graphite bearing zone is exposed south of the old pit and consists of a strongly foliated, rusty, pyrrhotite-graphite bearing fine-grained metaargillitic rock. A lithochemical analysis of a sample taken in the outcrop shows a carbon content of 18.2% and 0.17% sulphur (Appendix A).



Figure 8. Ångmansgruvan.
Photo: Torbjörn Bergman.

Ekorrsvedsgruvan

Ekorrsvedsgruvan is located 5 km northeast of *Gamla Skrammelfallsgruvan* and comprises two small trial pits next to each other on a northeast–southwesterly striking line (fig. 9). The pits are 6 m × 4–6 m wide and 3–4 m deep (fig. 10a). Adjacent to the pits, there is a pile of rusty waste rock consisting of a fine-grained quartz-mica rich metasedimentary rock with small amounts of visible graphite and pyrrhotite.

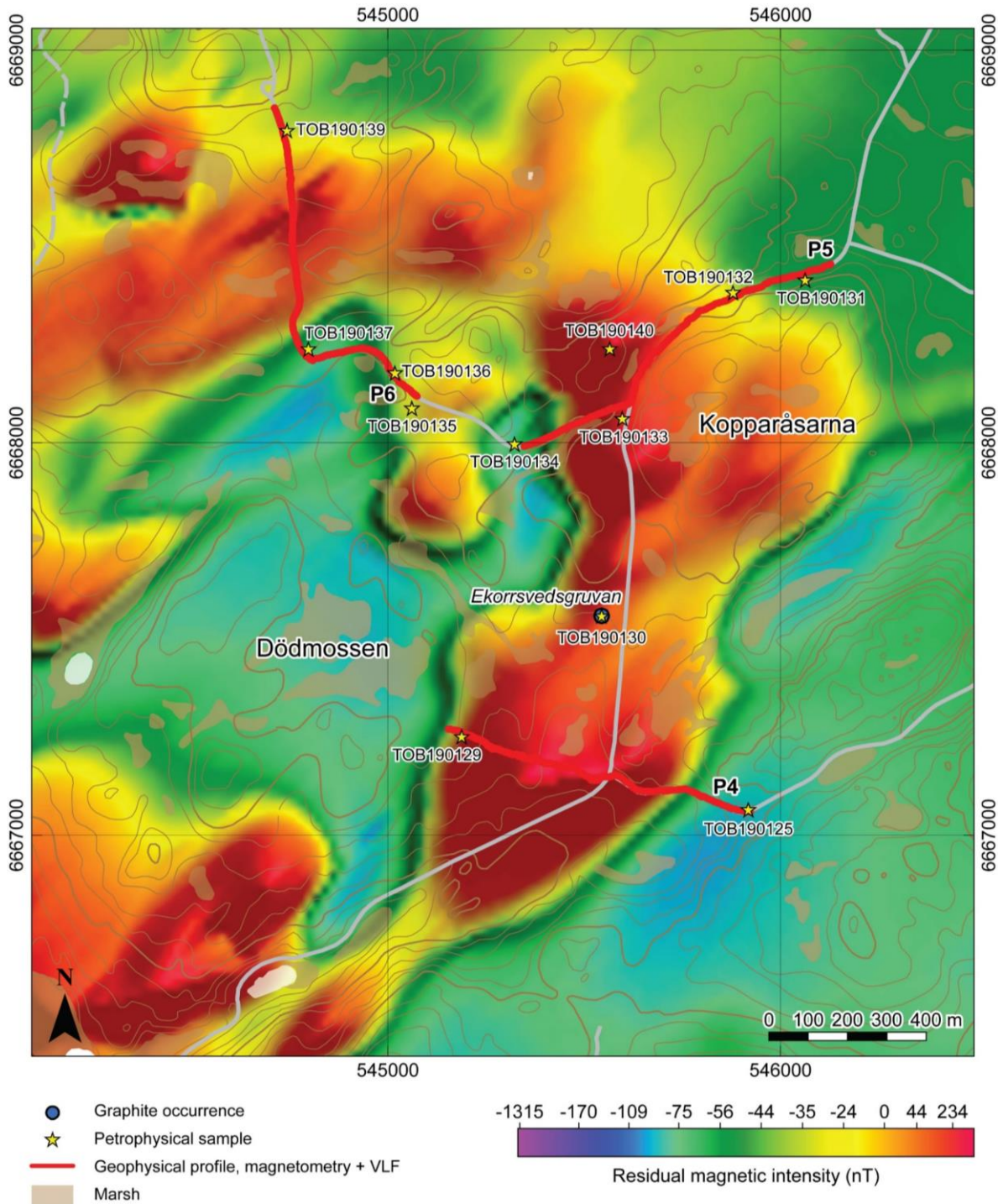


Figure 9. Residual magnetic field (see figure 3) in the area around Ekorrsvedsgruvan.

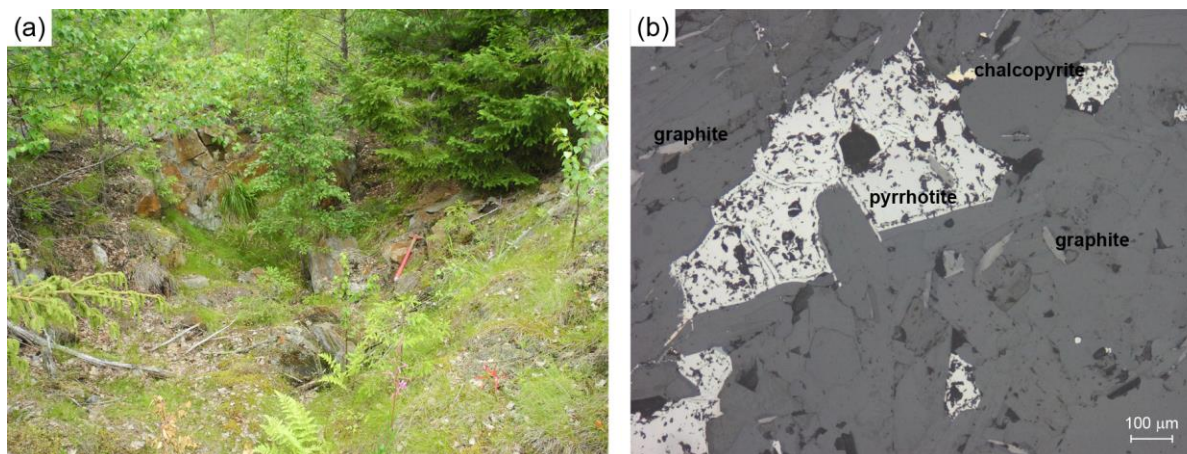


Figure 10. (a) Trial pit at Ekorrsvedsgruvan summer 2019. Photo taken towards north. **(b)** Microscope photo in reflected light of the typical graphite bearing quartz-mica dominated metasedimentary rock at Ekorrsvedsgruvan. Photos: Torbjörn Bergman.

Lithogeochemical analyses of samples from an outcrop in the southwestern pit and one sample from the waste dump show that the carbon content is only 1% (Appendix A). Microscope investigations of thin sections from the same samples show a presence of chalcopyrite and sphalerite, along with pyrrhotite and graphite, in a fine-grained matrix of quartz, muscovite and biotite (fig. 10b). The graphite, which constitutes 1–5% by volume of the samples, is amorphous and the individual grains are 0.1–0.2 mm in size. The *Ekorrsvedsgruvan* mine is situated near the maximum of a positive magnetic anomaly (fig. 9) as well as a resistivity low (fig. 4) which suggests that this graphite occurrence is part of a larger mineralised geological pyrrhotite-bearing horizon. The low carbon concentrations of the analysed rock samples, however, suggest that the anomalies are primarily due to pyrrhotite with little to no contribution from graphite.

The Styggberget area

In the Styggberget area, there are no known graphite occurrences. However, there is an operating garnet-quarry, the Styggberget quarry (fig. 11). The Styggberget quarry has been operating on and off since 2003 and is now run by Swegar AB which was recently granted a mining permission for an additional period of 20 years.

Garnet constitutes up to 20 % of the rock at Styggberget, which is a dark grey, fine- to medium grained, quartzo-feldspathic biotite-rich gneiss of disputable origin. Lundqvist & Hjelmqvist (1937) suggested an intrusive magmatic origin, mainly based on the presence of xenoliths of the surrounding metasedimentary rocks. A similar conclusion was made by Andersson et al. (2006) who also made a SIMS U–Pb age determination on zircon which yielded an age of 1894 ± 2 Ma. In contradiction to these authors, Strömberg (1983), who made the bedrock map of the area, included the garnet bearing rock type in the metasedimentary Larsbo formation.

The geophysical profile P9 in the current investigation is situated around 500 m east of the Styggberget quarry in an area with very few outcrops. Sampling of outcrops was only possible at three sites (fig. 11). The south–easternmost outcrop (TOB190156) consists of fine-grained, strongly lineated amphibolite, whereas the outcrop in the central part (TOB190157) consists of fine-grained metagreywacke and the north–westernmost outcrop is in a medium grained granodiorite (TOB190158). None of the outcrops contained visible amounts of garnets, graphite or pyrrhotite. Lithogeochemical analyses of the amphibolite and metagreywacke samples support this and did not show any elevated levels of carbon or sulphur.

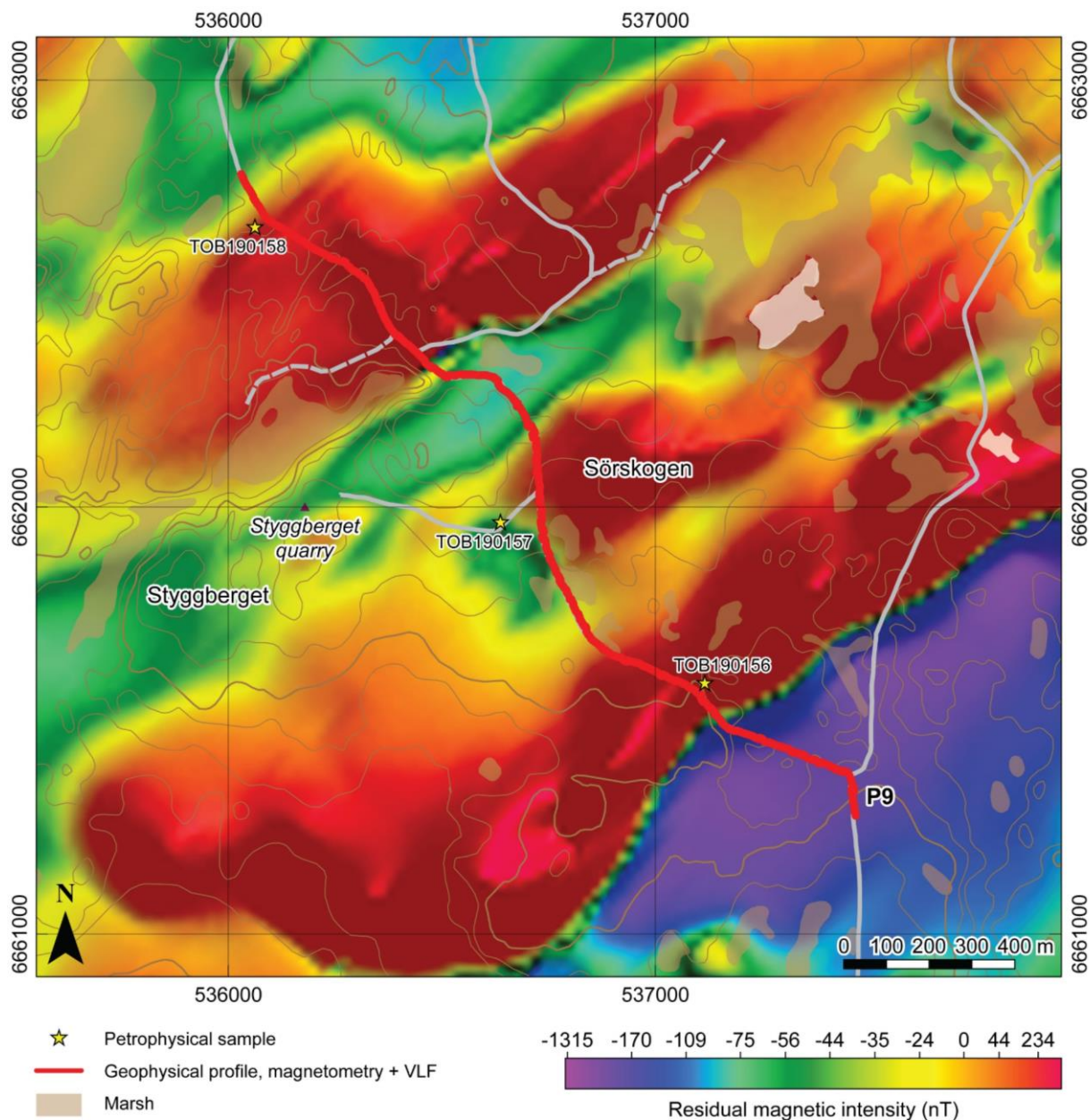


Figure 11. Residual magnetic field (see figure 3) in the Styggberget area.

PETROPHYSICAL PROPERTIES

Petrophysical properties were measured on a total of 42 bedrock samples from the area. Positioning was done with handheld GPS receiver. Measurements of density, magnetic susceptibility and natural remanent magnetisation were done at SGU, and the Koenigsberger ratio (Q) was estimated for all samples. The complete list of results can be found in *Appendix B. Petrophysical analysis results.*

Three of the samples have granodioritic–tonalitic composition, one of the samples consists of rhyolite, one of the samples consists of amphibolite, and the remaining samples consist of greywacke. A main trend appears in the relationship between density and magnetic susceptibility, where increasing density is associated with a small increase in magnetic susceptibility (fig. 12).

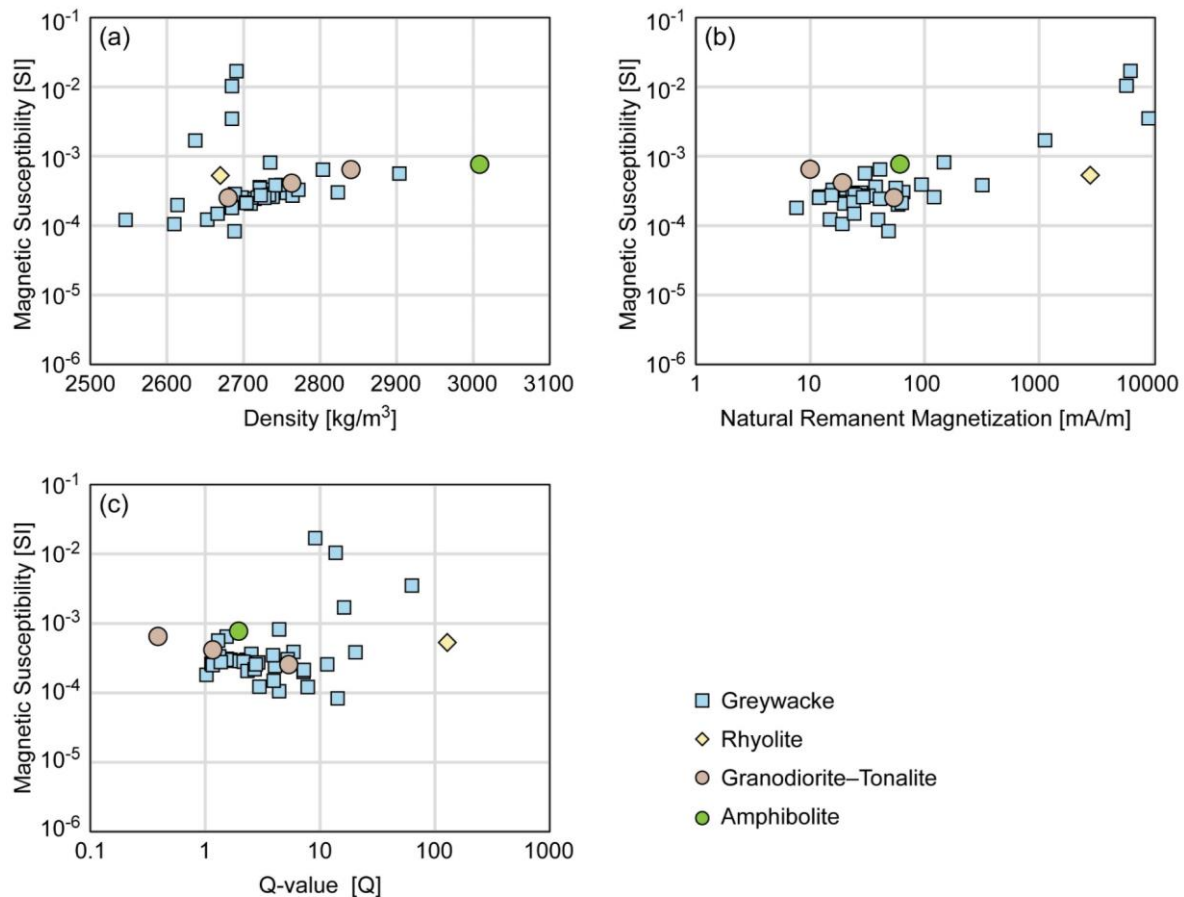


Figure 12. Results from petrophysical analysis of 48 bedrock samples in and around the Giltjärn-Skrammelfall area. Distribution of magnetic susceptibility versus (a) density, (b) natural remanent magnetisation, and (c) Q-value. The results are fully presented in Appendix B.

Most of the greywacke samples have densities in the range c. 2600–2800 kg/m³ and magnetic susceptibilities of less than 10^{-3} SI units and fall on the main trend. Four of the greywacke samples, however, form a second trend with significant increase in magnetic susceptibilities reaching nearly 1700×10^{-5} SI units while remaining in a low density range of c. 2650–2700 kg/m³. These four samples were taken from waste piles at *Gamla Skrammelfallsgruvan* and *Ekorrsvedsgruvan* (fig. 12a). These results are consistent with varying degree of pyrrhotite content in the greywacke. The samples of rhyolite and granodiorite-tonalite have typical densities in the range c. 2670–2840 kg/m³ and magnetic susceptibilities of less than 10^{-3} SI. The amphibolite sample (TOB190156A) has the highest density of all samples, c. 3009 kg/m³, and a magnetic susceptibility of c. 76×10^{-5} SI units, which is typical for amphibolite in that area.

The Q-value describes the relationship between the remanent and induced magnetisation, where Q-values above 1 indicate that the remanent magnetisation is dominant. Estimated Q-values for the 37 samples of greywacke lie in the range from 1 to 65 with an average of c. 6.6 (Appendix B). The three samples of granodiorite-tonalite have low values of natural remanent magnetisation (10–54 mA/m) and Q-values ranging from 0.4 to 5.4. The sample of rhyolite shows a natural remanent magnetisation of nearly 2800 mA/m, giving rise to the highest estimated Q-value of 131.4 (Appendix B). The amphibolite sample has a Q-value of 2.0. The results show that the measured magnetic intensities include significant contributions from remanent magnetisation in the rocks.

GEOPHYSICAL SURVEY, RESULTS AND DISCUSSION

During the 2019 survey, high-resolution measurements of magnetic field intensity and the electromagnetic field in the VLF-range (15–30 kHz) were done along nine profiles as shown in figures 6, 9 and 11. The equipment used was the GEM Systems GSM-19V combined magnetometer and triple-frequency VLF-sensor with GPS-positioning.

Five of the profiles run perpendicular across the anomalies in the Giltjärn-Skrammelfall area to obtain both higher resolution data over the known graphite-bearing horizons and more information about their subsurface geometry. A possible connection between the horizons in the Giltjärn and Skrammelfall mines was also investigated.

Figure 13 shows the variation of the electrical resistivity along profile P1, obtained from 2D inversion of the acquired VLF data. The profile passes several trial pits and mines in the Skrammelfall area. A clear correlation between known mineralisations and high electrical conductivity exists and suggests that electrically conductive rocks extend to depths of c. 50 m. However, because of the limited frequency range, the VLF method has limited sensitivity at depth below good conductors and in some cases the response from deeper parts do not reach the sensors at the surface. Therefore, the electrically conductive rocks might extend to even greater depths (e.g. the low resistivity feature in the range 200–300 m along profile).

Similarly, figure 14 shows the subsurface electrical resistivity variations along profile P8 which is located just north of Lake Norra Giltjärnen. The profile crosses both a projected extension of the horizon that hosts the Giltjärn mines as well as the band of high magnetic and low resistivity anomalies that may be the response from an extension of the graphite-bearing horizon found at the Skrammelfall mines (figures 4 and 6). The anomalies in the airborne magnetic and VLF data coincide for the most part with the topographic depression that hosts Lake Norra Giltjärnen and the surrounding wetlands. No good outcrops were available near the maxima of the anomalies that could be sampled for petrophysical and chemical analysis. The few samples taken in the vicinity of the anomalies did not show any traces of mineralisation and lithochemical analyses were not done on these. All of these samples have low densities ($<2770 \text{ kg/m}^3$) and magnetic susceptibilities ($<82 \times 10^{-5}$ SI units).

The resistivity section from 2D inversion of ground VLF data (fig. 14e) shows a distinct decrease in electrical resistivity down to depths of c. 100 m at both c. 200–300 m distance and 450–500 m distance along the profile. Because of the coincident high magnetic anomaly observed around 200 m distance along the profile (fig. 14a), which is of similar magnitude as the magnetic response at *Gamla Skrammelfallsgruvan* (see Fig. 13a), the response is likely caused by mineralised rock. The inferred connection from the regional geophysical maps, between this location and the Skrammelfall mines (figures 4 and 6), suggests that graphite-bearing rock and the associated pyrrhotite mineralisation may be present and responsible for the geophysical signature here. The resistivity anomaly around 450–500 m distance along the profile does not coincide with a magnetic anomaly (fig. 14), indicating that no pyrrhotite is present. A topographic lineament is observed between this location and the Giltjärn mines. This suggests a link with the Giltjärn mines but indicates that the VLF response at this location is caused by water-bearing fractures in a shear zone. However, this remains unclear at this stage and needs more thorough investigations and sampling through e.g. drilling.

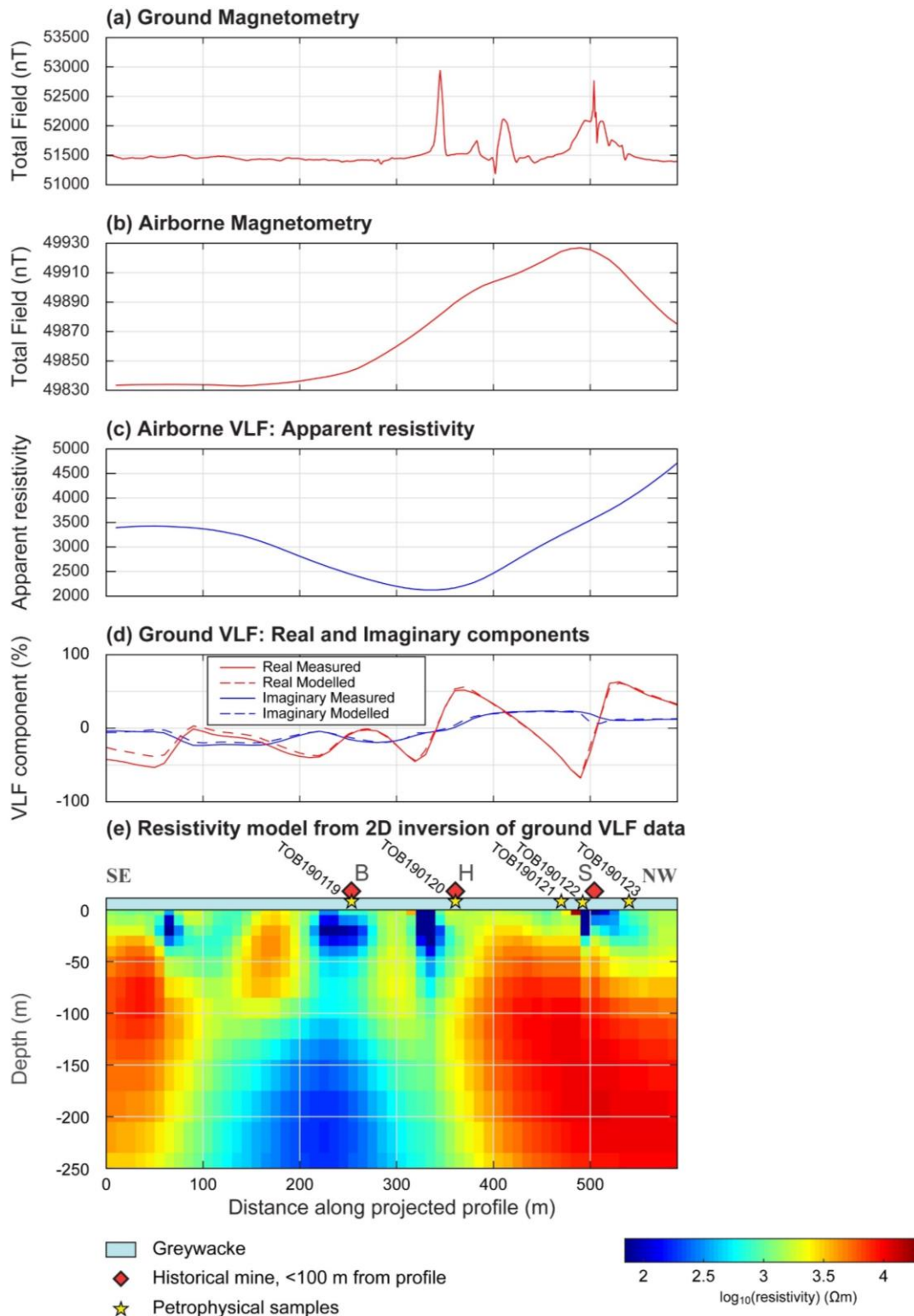


Figure 13. (a) Magnetic intensity along surface profile P1. (b) Magnetic intensity based on aeromagnetic measurements. (c) Apparent resistivity based on airborne VLF measurements. (d) Real and imaginary components of the VLF measurements along the surface profile. (e) Electrical resistivity at depth beneath the Skrammelfall mines, resulting from 2D inverse modelling of ground VLF-data along profile P1 (see figures 4 and 6). Low resistivity anomalies (blue colours) indicate good electrical conductivity in the subsurface. Historical mines located less than 100 m perpendicular distance from the profile have been projected to the surface of the section. The profile passes within a few tens of meters from the Blyertsgruvan (B), Haggrensgruvan (H) and Gamla Skrammelfallsgruvan (S) mines. Their locations, projected to the section and indicated by red diamonds, coincides with good electrical conductors that are seen to extend to depths of about 50 m.

The known graphite occurrence at *Ekorrsvedsgruvan* in the northeastern part is also located in an area with an anomaly in the magnetic and resistivity maps (figures 3 and 4), suggesting that the geophysical anomalies delineate a potentially pyrrhotite and graphite bearing horizon. Geophysical surveying and sampling of bedrock was therefore done along three profiles perpendicular to the anomalies in this area. Inversion of ground based VLF data along these profiles suggest electrically conductive material to extend to c. 50 m depth in a few locations. Due to lack of outcrops, only few rock samples could be taken near the maxima of these anomalies (fig. 9). None of these, and none of samples taken elsewhere along the profiles, showed any visible amounts of graphite. The lithochemical analyses of samples from *Ekorrsvedsgruvan* revealed only weakly elevated concentrations of carbon (maximum 1.2%, Appendix A) which suggests that the geophysical anomalies are primarily due to pyrrhotite with little to no contribution from graphite. This is further supported by the microscopic investigation of samples from *Ekorrsvedsgruvan* (fig. 10b) which shows a high concentration of pyrrhotite but only minor amounts of graphite.

Areas to the west and northwest of the known graphite occurrences nearby the Giltjärn and Skrammelfall mines have geophysical anomalies similar to those near *Ekorrsvedsgruvan*. Some of the strongest magnetic and VLF anomalies which also correlate with the dominant gravity anomaly in the study area (fig. 5) were targeted by profile P9 (fig. 11). Bedrock samples from this profile, although very limited in number and geographical distribution, did not show any presence of graphite or elevated concentrations of carbon (samples TOB190156A and TOB190157A in Appendix A). Hence, no indication that graphite mineralisation of significant concentrations extends beyond the Giltjärn–Skrammelfall area were encountered.

The sampled amphibolite outcrop in the Styggberget area (TOB190156; fig. 11), shows that mafic bodies that have not previously been mapped occur in the area. Minor intrusions of gabbro are however known from places northwest and southeast of the Styggberget area (fig. 2) and it is therefore not unlikely to assume the presence of an unexposed mafic intrusion at depth, which could explain the large gravity anomaly in this area (fig. 5). Such an intrusion could also have played an important role as a heat source for metamorphism and the formation of the garnet-bearing rock mined in the Styggberget quarry. The low resistivity anomaly near TOB190156 appears to coincide with a topographic lineament which suggests that VLF response is related to water-bearing fractures in shear zones that crosscut the area.

CONCLUSIONS

This investigation, focusing on the area northwest of Norberg with historic mining of graphite, shows a continued potential for graphite exploration.

The regional geophysical data, acquired by airborne measurements in 2016, show that the known occurrences at Giltjärn and Skrammelfall mines lie in areas of southwest–northeasterly striking anomalies of elevated magnetic intensity and electrically conductivity. Lithochemical samples from outcrops and waste rock nearby the old Skrammelfall mines show graphite-bound carbon concentrations of up to nearly 32%. In addition, results from inversion of electromagnetic data show that the electrically conductive rock that host the graphite may continue to depths of about 50 m (fig. 13). The deepest mine in the area, *Gamla Skrammelfallsgruvan*, was earlier mined to c. 20 m depth. Samples retrieved from outcrops and waste rock at the Giltjärn mines show carbon concentrations of up to c. 20%. Here, the electrically conductive rocks may be inferred to depths of as much as 100 m.

The magnetic and resistivity anomalies at the Skrammelfall mines appear to continue beneath Lake Norra Giltjärnen and the surrounding wetlands and are parallel with the anomalies associated with the Giltjärn mines. Inversion of ground based VLF data, both along a profile near the Giltjärn mines and one directly in between the two mining areas (fig. 14), indicates that this anomaly is caused by electrically conductive rocks that may extend to depths of c. 100 m. However, a lack of good outcrop prevented sampling at the anomaly and a few samples could only be taken in the vicinity where no traces of mineralisation were observed.

The geophysical results indicate that the conductive rocks in the *Ekorrsvedsgruvan* area may continue to depths of c. 50 m. However, only minor amounts of graphite were observed in outcrops and samples, and lithochemical analyses of samples from the *Ekorrsvedsgruvan* trial pit show carbon concentrations of c. 1%. The noted abundance of pyrrhotite in waste rock and outcrop at *Ekorrsvedsgruvan* and the surrounding area suggests that pyrrhotite is mainly responsible for the geophysical anomalies.

In the Styggberget area, slightly to the west of the Giltjärn and Skrammelfall mines, a magnetometry and VLF profile was measured across an area with strong geophysical anomalies. Only a few samples could be taken, and lithochemical analyses showed only trace amounts of carbon and sulphur. Amphibolite was encountered in one outcrop and minor gabbro intrusions are known directly to the northwest and the southeast of the area. Together with the major gravity anomaly and anomalies in aeromagnetic and resistivity data, this suggests that the area hosts a large mafic intrusion. The area is intersected by several shear zones.

Sampling of rock that can be directly tied to the geophysical anomalies, e.g. via drilling, would shed light on the cause of the geophysical response in the area. The Giltjärn–Skrammelfall area, where graphite is a known major component of the rock and directly linked to the anomalies in several locations, probably has the largest potential for graphite exploration and extraction among the investigated areas.

REFERENCES

- Andersson, U. B., Högdahl, K., Sjöström, H. & Bergman, S., 2006: Multistage growth and reworking of the Palaeoproterozoic crust in the Bergslagen area, southern Sweden: evidence from U-Pb geochronology. *Geological Magazine* 143, 679–697.
- Ambros, M., 1986a: Berggrundskartan 12G Avesta NV. *Sveriges geologiska undersökning Af 152*.
- Ambros, M., 1986b: Berggrundskartan 12G Avesta SV. *Sveriges geologiska undersökning Af 153*.
- Bergman, T., Hellström, F., Hildebrand, L., Larsson, D & Söderhielm, J., in prep: Mineralresursinventering i Västmanlands län och Heby kommun, Uppsala län. SGU-rapport, Sveriges geologiska undersökning.
- Claesson, D., Bakker, E., Bergman, T., Hallberg, A., Hedin, P., Jönberger, J., Ladenberger, A., Lewerentz, A., Morris, G., Reginiussen, H., Ripa, M. & Wedmark, M., 2020: Rapportering av regeringsuppdrag: Innovationskritiska metaller och mineral i Bergslagen. RR 2020:02, Sveriges geologiska undersökning, 77 pp.
- Claesson, S., Huhma, H., Kinny, P.D. & Williams, I. S., 1993: Svecofennian detrital zircon ages – implications for the Precambrian evolution of the Baltic shield. *Precambrian Research* 64, 109–130.
- Geijer, P., 1936: Norbergs berggrund och malmfyndigheter. *Sveriges geologiska undersökning Ca 24*, 162 pp.
- Hjelmqvist, S., 1938: Über Sedimentgesteine in der Leptitformation Mittelschwedens. Die sogenannte "Larsboerie". *Sveriges geologiska undersökning C 413*, 39 pp.
- Lindroth, G.T., 1918: Grafitfyndigheterna inom Norbergs Bergslag. *Geologiska Föreningen i Stockholm Förhandlingar* 40, 27–76.
- Lundqvist, G. & Hjelmqvist, S. 1937: Beskrivning till kartbladet Smedjebacken. *Sveriges geologiska undersökning Aa 181*, 129 pp.
- Mogensen, F. 1934: De geologiska förhållandena vid grafitförekomsterna i Norberg. *Geologiska föreningens i Stockholm förhandlingar* 56, 7 pp.
- Stephens, M.B. & Jansson, N.F., 2020: Paleoproterozoic (1.9–1.8 Ga) syn-orogenic magmatism, sedimentation and mineralization in the Bergslagen lithotectonic unit, Svecokarelian orogen. In: M.B. Stephens & J. Bergman Weihed (eds.) 2020. *Sweden: Lithotectonic Framework, Tectonic Evolution and Mineral Resources*. Geological Society, London, Memoirs 50, 155–206.
- Stephens, M.B., Ripa, M., Lundström, I., Persson, L., Bergman, T., Ahl, M., Wahlgren, C.-H., Persson, P.-O. & Wickström, L., 2009: Synthesis of the bedrock geology in the Bergslagen region, Fennoscandian Shield, south-central Sweden. *Sveriges geologiska undersökning Ba 58*, 259 pp.
- Strömberg, A 1983: Berggrundskartan 12F Ludvika SO. *Sveriges geologiska undersökning Af 128*.
- Strömberg, A. 1996: Berggrundskartan 12F Ludvika NO. *Sveriges geologiska undersökning Af 174*.
- Tegengren, F.R., 1924: Sveriges äldre malmer och bergverk., *Sveriges geologiska undersökning Ca 17*, 406 pp.
- Törnebohm, A. E., 1875: Om lagerföljden inom Norbergs malmfält. *Geologiska Föreningen i Stockholm Förhandlingar* 2, 329 pp.

APPENDIX A. LITHOGEOCHEMICAL ANALYSIS RESULTS

Methods

Lithogeochemical analyses were conducted at ALS Minerals in 2018 & 2019 using analytical packages referred to as ME-ICP06, ME-MS81, ME-MS41, ME-MS42, ME-4ACD81, IR-07, IR08 and ICP23. ALS method code refers to analytical method used for each element and is described in ALS methodology factsheets at <http://www.alsglobal.com>.

Sample preparation was carried out by ALS Minerals in Piteå (Sweden) and subsequent analytical work performed at ALS Minerals lab in Ireland. Preparation involved crushing of the sample and pulverising it to a powder using low-chrome steel grinding mills.

Table A1–A3 contain the complete set of lithogeochemical analysis results of samples from mine waste material and outcrops with graphite bearing metasedimentary rocks in and around the Giltjärn-Skrammelfall area northwest of Norberg.

Table A1. Samples TOB190130A, TOB190130B, TOB190119A, TOB190119B, TOB190119C and TOB180252A.

Sample ID			TOB190130A	TOB190130B	TOB190119A	TOB190119B	TOB190119C	TOB180252A
Easting (SWEREF99TM)			545545	545545	542806	542806	542806	542803
Northing (SWEREF99TM)			6667559	6667559	6663121	6663121	6663121	6663125
Sample type			Waste rock	Outcrop	Waste rock	Waste rock	Waste rock	Waste rock
Location			<i>Ekorrsvedsgruvan</i>	<i>Ekorrsvedsgruvan</i>	<i>Blyertsgruvan</i>	<i>Blyertsgruvan</i>	<i>Blyertsgruvan</i>	<i>Blyertsgruvan</i>
C	C-IR07	%	1	1.23	0.8	31.7	0.04	0.23
S	S-IR08	%	1.59	1.65	0.34	0.23	0.04	0.03
SiO2	ME-ICP06	%	66.4	61.3	43.9	36.9	62.7	68.7
Al2O3	ME-ICP06	%	16.3	15.7	20.5	13.05	18.8	16.75
Fe2O3	ME-ICP06	%	5.99	7.58	12.15	3.65	5.86	5.18
CaO	ME-ICP06	%	1.48	1.44	2.78	1.64	0.48	0.83
MgO	ME-ICP06	%	1.93	2.34	6.9	1.26	2.26	1.69
Na2O	ME-ICP06	%	1.96	2.15	2.26	2.88	1.28	1.74
K2O	ME-ICP06	%	3.53	3.33	5.19	2.6	4.88	3.64
Cr2O3	ME-ICP06	%	0.015	0.016	0.023	0.009	0.016	0.018
TiO2	ME-ICP06	%	0.53	0.59	1.66	0.39	0.63	0.56
MnO	ME-ICP06	%	0.03	0.03	0.09	0.02	0.04	0.04
P2O5	ME-ICP06	%	0.08	0.07	0.31	0.07	0.08	0.09
SrO	ME-ICP06	%	0.02	0.02	0.01	0.02	<0.01	<0.01
BaO	ME-ICP06	%	0.08	0.06	0.05	0.03	0.08	0.05
Ba	ME-MS81	ppm	677	538	456	276	737	450
Ce	ME-MS81	ppm	94.4	81	37.5	43.1	98.6	86.2
Cr	ME-MS81	ppm	100	110	140	60	90	80
Cs	ME-MS81	ppm	5.82	7.88	30	7.13	10.95	6.33
Dy	ME-MS81	ppm	5.07	5.83	3.91	2.53	5.27	4.93
Er	ME-MS81	ppm	3.01	3.48	2.92	1.39	3.02	2.62
Eu	ME-MS81	ppm	1.14	1.2	0.97	0.97	1.29	1.46
Ga	ME-MS81	ppm	22.3	21	36.6	16.8	30.3	22.3
Gd	ME-MS81	ppm	6.92	6.1	4.61	2.64	6.29	4.82
Hf	ME-MS81	ppm	3.7	3.8	3.1	3	4.9	5.6
Ho	ME-MS81	ppm	0.96	1.15	0.77	0.4	0.9	0.81
La	ME-MS81	ppm	51.4	41.7	17.5	21.6	49.7	42.6
Lu	ME-MS81	ppm	0.44	0.55	0.22	0.08	0.26	0.35
Nb	ME-MS81	ppm	12.3	12.1	12.3	6.5	14.6	13.6
Nd	ME-MS81	ppm	43.9	38	21	20	45.3	37.7
Pr	ME-MS81	ppm	11.75	10.25	4.72	5.02	11.3	9.59
Rb	ME-MS81	ppm	146	152	385	152	233	156.5
Sm	ME-MS81	ppm	8.03	7.16	4.77	3.36	7.79	6.56
Sn	ME-MS81	ppm	3	3	2	<1	3	3
Sr	ME-MS81	ppm	228	249	195.5	214	122	181
Ta	ME-MS81	ppm	1.1	1	0.3	<0.1	0.9	0.9
Tb	ME-MS81	ppm	0.89	0.9	0.54	0.23	0.83	0.83
Th	ME-MS81	ppm	16.85	14.85	1.86	8.27	16.65	13.5
Tm	ME-MS81	ppm	0.4	0.48	0.29	0.09	0.34	0.38
U	ME-MS81	ppm	6.11	4.93	1.53	2.38	4.23	3.66
V	ME-MS81	ppm	245	244	288	58	141	95
W	ME-MS81	ppm	5	5	2	1	3	3
Y	ME-MS81	ppm	26.9	33.4	24.3	15.4	28.9	24
Yb	ME-MS81	ppm	2.88	3.62	2.44	1.48	2.95	2.22
Zr	ME-MS81	ppm	159	142	115	112	168	182
As	ME-MS42	ppm	1.5	2.4	0.7	3.7	16.7	2.9
Bi	ME-MS42	ppm	0.77	0.53	0.23	0.57	0.56	0.27
Hg	ME-MS42	ppm	0.007	<0.005	<0.005	<0.005	<0.005	0.009
Sb	ME-MS42	ppm	0.08	0.08	0.13	0.21	0.11	<0.05
Se	ME-MS42	ppm	5.7	9.4	1.1	0.9	0.4	0.4
Te	ME-MS42	ppm	0.26	0.35	0.04	0.07	0.05	0.03
LOI	OA-GRA05	%	3.28	5.26	3.81	35.7	3.24	2.39
Total	TOT-ICP06	%	101.63	99.89	99.63	98.22	100.35	101.68
Ag	ME-4ACD81	ppm	<0.5	0.5	0.5	<0.5	<0.5	<0.5
Cd	ME-4ACD81	ppm	<0.5	<0.5	<0.5	<0.5	<0.5	<0.5
Co	ME-4ACD81	ppm	13	14	16	1	14	9
Cu	ME-4ACD81	ppm	163	233	79	38	22	13
Mo	ME-4ACD81	ppm	23	18	2	1	1	2
Ni	ME-4ACD81	ppm	201	209	13	9	36	27
Pb	ME-4ACD81	ppm	13	11	26	19	20	20
Sc	ME-4ACD81	ppm	8	10	35	10	17	14

Table A1. Continuation.

Sample ID			TOB190130A	TOB190130B	TOB190119A	TOB190119B	TOB190119C	TOB180252A
Easting (SWEREF99TM)			545545	545545	542806	542806	542806	542803
Northing (SWEREF99TM)			6667559	6667559	6663121	6663121	6663121	6663125
Sample type			Waste rock	Outcrop	Waste rock	Waste rock	Waste rock	Waste rock
Location			<i>Ekorrsvedsgruvan</i>	<i>Ekorrsvedsgruvan</i>	<i>Blyertsgruvan</i>	<i>Blyertsgruvan</i>	<i>Blyertsgruvan</i>	<i>Blyertsgruvan</i>
Zn	ME-4ACD81	ppm	126	117	216	34	122	71
Ag	ME-MS41	ppm	0.26	0.36	0.18	0.28	0.08	0.04
Al	ME-MS41	%	1.5	1.95	6.04	1.42	2.68	2.02
As	ME-MS41	ppm	1.5	2.4	0.7	3.8	16.9	2.7
Au	ME-MS41	ppm	<0.02	<0.02	<0.02	<0.02	<0.02	<0.02
B	ME-MS41	ppm	<10	<10	<10	<10	<10	<10
Ba	ME-MS41	ppm	100	90	360	70	150	80
Be	ME-MS41	ppm	0.21	0.32	0.61	0.42	1.02	0.66
Bi	ME-MS41	ppm	0.75	0.51	0.22	0.55	0.54	0.29
Ca	ME-MS41	%	0.09	0.06	0.41	0.12	0.05	0.12
Cd	ME-MS41	ppm	0.21	0.23	0.17	0.12	0.05	0.07
Ce	ME-MS41	ppm	37.7	32.4	20.2	34.9	79.2	65.6
Co	ME-MS41	ppm	14	16.2	16.2	3	12.3	8.8
Cr	ME-MS41	ppm	40	61	143	57	52	51
Cs	ME-MS41	ppm	4.8	6.69	27.4	4.96	9.78	5.92
Cu	ME-MS41	ppm	170	231	80.1	34.4	21.8	11.3
Fe	ME-MS41	%	4.28	5.43	8.52	2.68	4.02	3.49
Ga	ME-MS41	ppm	5.31	7.08	24.9	7.19	8.77	6.92
Ge	ME-MS41	ppm	0.07	0.12	0.4	0.06	0.11	0.16
Hf	ME-MS41	ppm	0.33	0.22	0.38	0.26	0.51	0.33
Hg	ME-MS41	ppm	<0.01	<0.01	<0.01	<0.01	<0.01	0.01
In	ME-MS41	ppm	0.023	0.024	0.076	0.019	0.025	0.021
K	ME-MS41	%	0.99	1.23	3.93	0.59	1.69	0.91
La	ME-MS41	ppm	20.2	17.2	9.1	17	40.3	33.1
Li	ME-MS41	ppm	22.9	29.1	124	29.5	52.1	62.2
Mg	ME-MS41	%	1.06	1.32	4.12	0.71	1.24	0.86
Mn	ME-MS41	ppm	218	216	578	122	302	275
Mo	ME-MS41	ppm	23.8	18	0.9	0.83	0.67	0.81
Na	ME-MS41	%	0.04	0.04	0.18	0.03	0.06	0.04
Nb	ME-MS41	ppm	0.24	0.27	0.35	0.3	0.38	0.46
Ni	ME-MS41	ppm	208	210	15	10	35.5	25.8
P	ME-MS41	ppm	290	260	1380	350	300	410
Pb	ME-MS41	ppm	3.7	4.6	8.9	13.1	6.2	6.2
Rb	ME-MS41	ppm	73.1	92.3	326	49.5	129.5	76.3
Re	ME-MS41	ppm	0.037	0.029	0.001	0.002	0.002	0.001
S	ME-MS41	%	1.79	1.9	0.37	0.26	0.04	0.05
Sb	ME-MS41	ppm	0.08	0.08	0.13	0.21	0.11	0.05
Sc	ME-MS41	ppm	1.8	4.3	40	7.7	4.8	4.4
Se	ME-MS41	ppm	5.7	9.4	1.1	0.9	0.4	0.3
Sn	ME-MS41	ppm	0.5	0.7	2.2	0.5	1.1	0.8
Sr	ME-MS41	ppm	3.9	6.9	11.1	3.7	3.8	3.6
Ta	ME-MS41	ppm	<0.01	<0.01	0.01	<0.01	<0.01	<0.01
Te	ME-MS41	ppm	0.26	0.35	0.04	0.07	0.05	0.02
Th	ME-MS41	ppm	7	6	1	7.8	13.6	10.5
Ti	ME-MS41	%	0.123	0.158	0.565	0.104	0.242	0.175
Tl	ME-MS41	ppm	0.72	0.94	2.16	0.43	0.87	0.57
U	ME-MS41	ppm	4.39	2.64	0.83	1.59	3.11	2.63
V	ME-MS41	ppm	77	106	278	61	62	39
W	ME-MS41	ppm	0.37	0.35	0.39	0.09	0.17	0.13
Y	ME-MS41	ppm	6.23	4.55	11.2	6.08	6.66	8.29
Zn	ME-MS41	ppm	120	109	198	31	114	71
Zr	ME-MS41	ppm	11.8	7.9	16.5	8.6	18.1	11.5
Au	PGM-ICP23	ppm	0.004	0.001	<0.001	0.011	0.001	0.004
Pt	PGM-ICP23	ppm	<0.005	<0.005	<0.005	<0.005	<0.005	<0.005
Pd	PGM-ICP23	ppm	0.008	0.013	0.001	0.003	0.004	0.002
Li	ME-4ACD81	ppm	30	40	130	30	60	60
Tl	ME-MS42	ppm	0.72	0.94	2.16	0.43	0.87	0.57
Ge	ME-MS81	ppm	<5	<5	<5	<5	<5	<5
In	ME-MS42	ppm	0.023	0.024	0.076	0.019	0.025	0.021
Re	ME-MS42	ppm	0.037	0.029	0.001	0.002	0.002	0.001

Table A2. Samples TOB180251B, TOB190122A, TOB190122B, TOB180245A, TOB180245B and TOB180245C.

Sample ID			TOB180251B	TOB190122A	TOB190122B	TOB180245A	TOB180245B	TOB180245C
Easting (SWEREF99TM)			542778	542678	542678	542661	542661	542661
Northing (SWEREF99TM)			6663208	6663322	6663322	6663317	6663317	6663317
Sample type			Waste rock	Waste rock	Waste rock	Waste rock	Waste rock	Waste rock
Location			<i>Haggrensgruvan</i>	<i>Gamla Skrammelfallsgruvan 1</i>				
C	C-IR07	%	0.23	28.3	22.2	27.8	26	29.7
S	S-IR08	%	0.04	4.3	5	4.3	6.58	6.21
SiO2	ME-ICP06	%	69.9	26.3	42.4	37	33.4	32.9
Al2O3	ME-ICP06	%	15.35	6.64	9.34	10.35	11.55	10.25
Fe2O3	ME-ICP06	%	3.63	7.26	12.1	11.1	16.25	15.6
CaO	ME-ICP06	%	1.18	0.37	0.58	0.53	0.45	0.54
MgO	ME-ICP06	%	1.66	1.06	1.43	1.48	1.64	1.6
Na2O	ME-ICP06	%	1.6	0.4	0.66	0.45	0.26	0.55
K2O	ME-ICP06	%	4.31	1.87	2.59	2.86	3.25	2.65
Cr2O3	ME-ICP06	%	0.013	0.012	0.016	0.016	0.022	0.02
TiO2	ME-ICP06	%	0.52	0.33	0.45	0.47	0.53	0.47
MnO	ME-ICP06	%	0.03	0.02	0.02	0.02	0.02	0.03
P2O5	ME-ICP06	%	0.05	0.09	0.17	0.19	0.19	0.13
SrO	ME-ICP06	%	0.02	<0.01	<0.01	<0.01	<0.01	<0.01
BaO	ME-ICP06	%	0.06	0.02	0.03	0.03	0.04	0.03
Ba	ME-MS81	ppm	597	261	220	300	361	288
Ce	ME-MS81	ppm	63.4	54.7	37.8	57	71.1	43.9
Cr	ME-MS81	ppm	80	80	90	100	150	140
Cs	ME-MS81	ppm	4.07	5.55	5.3	4.77	4.49	3.6
Dy	ME-MS81	ppm	4.32	5.03	5.12	5.96	7.5	5.98
Er	ME-MS81	ppm	2.72	3.49	3.65	3.89	4.98	3.77
Eu	ME-MS81	ppm	1.4	1	1	1.05	0.85	1.13
Ga	ME-MS81	ppm	16.8	15.3	12.6	17.9	16.8	15
Gd	ME-MS81	ppm	4.79	5.31	5.03	5.94	6.07	5.09
Hf	ME-MS81	ppm	7.3	3	2.8	3.6	4.4	4.2
Ho	ME-MS81	ppm	0.94	0.93	1.05	1.34	1.58	1.15
La	ME-MS81	ppm	35.8	32.4	21.3	30.5	41.7	26.3
Lu	ME-MS81	ppm	0.36	0.54	0.65	0.8	1.05	0.68
Nb	ME-MS81	ppm	10.9	8.5	8.1	12.1	16.2	8.9
Nd	ME-MS81	ppm	30.1	28.6	21.1	30.1	33.3	26
Pr	ME-MS81	ppm	8.04	7.27	5.53	7.43	9.59	6.82
Rb	ME-MS81	ppm	182	118	109	121.5	127	107.5
Sm	ME-MS81	ppm	5.75	5.57	5.07	6.21	6.27	5.83
Sn	ME-MS81	ppm	3	3	2	3	4	4
Sr	ME-MS81	ppm	161	51.2	55.5	42.9	21.4	50.7
Ta	ME-MS81	ppm	1	<0.1	0.6	0.6	1.7	0.7
Tb	ME-MS81	ppm	0.63	0.67	0.83	1.01	0.96	0.82
Th	ME-MS81	ppm	12.9	8.21	8.91	12.7	12.45	10.7
Tm	ME-MS81	ppm	0.37	0.44	0.45	0.63	0.81	0.58
U	ME-MS81	ppm	3.02	17	17.5	19.5	24.7	11.5
V	ME-MS81	ppm	80	633	699	832	878	821
W	ME-MS81	ppm	2	7	7	10	10	7
Y	ME-MS81	ppm	23.7	33.5	30	34.4	43.3	34.7
Yb	ME-MS81	ppm	2.61	3.78	3.94	4.94	5.86	3.71
Zr	ME-MS81	ppm	242	109	104	120	158	128
As	ME-MS42	ppm	23	1.7	5.4	2.9	46.1	2.4
Bi	ME-MS42	ppm	0.13	3.17	2.15	1.78	2.67	3.29
Hg	ME-MS42	ppm	<0.005	<0.005	0.178	0.005	0.007	<0.005
Sb	ME-MS42	ppm	0.05	0.62	0.44	0.36	0.37	0.53
Se	ME-MS42	ppm	0.3	19.6	22.6	18	25.7	24.8
Te	ME-MS42	ppm	0.02	0.46	0.41	0.38	0.63	0.54
LOI	OA-GRA05	%	2.75	32.8	29.6	34.3	31.7	35.7
Total	TOT-ICP06	%	101.07	77.17	99.39	98.8	99.3	100.47
Ag	ME-4ACD81	ppm	<0.5	1.9	1.9	1.2	1.6	1.7
Cd	ME-4ACD81	ppm	<0.5	10.2	1.2	3.6	9.9	4.6
Co	ME-4ACD81	ppm	4	21	15	22	17	22
Cu	ME-4ACD81	ppm	12	381	453	204	261	404
Mo	ME-4ACD81	ppm	2	81	65	77	84	77
Ni	ME-4ACD81	ppm	40	399	456	373	598	587
Pb	ME-4ACD81	ppm	5	23	18	15	14	15
Sc	ME-4ACD81	ppm	9	13	11	13	15	13

Table A2. Continuation.

Sample ID	TOB180251B	TOB190122A	TOB190122B	TOB180245A	TOB180245B	TOB180245C		
Easting (SWEREF99TM)	542778	542678	542678	542661	542661	542661		
Northing (SWEREF99TM)	6663208	6663322	6663322	6663317	6663317	6663317		
Sample type	Waste rock	Waste rock	Waste rock	Waste rock	Waste rock	Waste rock		
Location	<i>Haggrensgruvan</i>	<i>Gamla Skrammelfallsgruvan 1</i>						
Zn	ME-4ACD81	ppm	69	925	166	362	866	421
Ag	ME-MS41	ppm	0.06	1.74	1.74	1.42	1.89	1.97
Al	ME-MS41	%	1.48	1.09	1.05	1.03	1.03	1.07
As	ME-MS41	ppm	21.9	1.7	5.5	2.7	43.9	2.3
Au	ME-MS41	ppm	<0.02	<0.02	<0.02	<0.02	<0.02	<0.02
B	ME-MS41	ppm	10	<10	<10	<10	<10	<10
Ba	ME-MS41	ppm	20	30	30	20	20	10
Be	ME-MS41	ppm	1.08	0.46	0.43	0.54	0.54	0.72
Bi	ME-MS41	ppm	0.16	3.13	2.12	1.84	2.75	3.38
Ca	ME-MS41	%	0.52	0.23	0.24	0.27	0.28	0.25
Cd	ME-MS41	ppm	0.06	10.2	1.36	3.38	9.97	4.56
Ce	ME-MS41	ppm	46.3	55.8	38.7	50.1	60.5	38
Co	ME-MS41	ppm	4.8	23	15.1	23.1	18.8	21.6
Cr	ME-MS41	ppm	39	46	40	38	35	41
Cs	ME-MS41	ppm	1.24	4.27	4.05	3.09	3.03	2
Cu	ME-MS41	ppm	10.5	368	466	202	266	413
Fe	ME-MS41	%	2.33	8.01	9.16	7.77	11.35	11.15
Ga	ME-MS41	ppm	5.89	3.9	3.61	3.5	3.56	3.68
Ge	ME-MS41	ppm	0.15	0.26	0.24	0.23	0.33	0.35
Hf	ME-MS41	ppm	0.64	0.45	0.5	0.38	0.57	0.35
Hg	ME-MS41	ppm	<0.01	<0.01	0.17	0.01	0.01	0.01
In	ME-MS41	ppm	0.01	0.084	0.014	0.036	0.087	0.041
K	ME-MS41	%	0.13	0.43	0.41	0.29	0.32	0.17
La	ME-MS41	ppm	23.7	32.8	22	27.3	33.6	20.9
Li	ME-MS41	ppm	34.2	28.2	25	31.2	30.9	33.5
Mg	ME-MS41	%	0.82	0.79	0.76	0.71	0.71	0.74
Mn	ME-MS41	ppm	186	179	170	162	151	181
Mo	ME-MS41	ppm	1.95	81	70.6	70.6	85	71.7
Na	ME-MS41	%	0.02	0.01	0.01	0.01	0.01	0.02
Nb	ME-MS41	ppm	0.41	0.15	0.2	0.17	0.13	0.16
Ni	ME-MS41	ppm	39	394	467	381	634	594
P	ME-MS41	ppm	260	600	750	870	950	530
Pb	ME-MS41	ppm	5.9	16	12.8	13.4	17.4	14.5
Rb	ME-MS41	ppm	9.1	39.8	34.6	26.9	27.9	15.2
Re	ME-MS41	ppm	0.001	0.186	0.158	0.173	0.198	0.167
S	ME-MS41	%	0.05	4.46	5.33	4.24	6.82	6.38
Sb	ME-MS41	ppm	0.08	0.62	0.44	0.39	0.4	0.56
Sc	ME-MS41	ppm	2.6	2.3	2	1.9	2	2
Se	ME-MS41	ppm	0.2	19.6	22.6	18.4	26.3	25.4
Sn	ME-MS41	ppm	0.7	0.6	0.5	0.6	0.5	0.5
Sr	ME-MS41	ppm	6.4	2.8	2.5	2.8	2.9	2.4
Ta	ME-MS41	ppm	<0.01	0.01	0.01	<0.01	<0.01	<0.01
Te	ME-MS41	ppm	0.01	0.46	0.41	0.34	0.58	0.49
Th	ME-MS41	ppm	11.8	9.6	8.7	10.5	11.5	10
Ti	ME-MS41	%	0.163	0.109	0.099	0.106	0.089	0.101
Tl	ME-MS41	ppm	0.1	1.43	1.12	0.75	0.89	0.92
U	ME-MS41	ppm	2.17	23.4	20.3	19.65	29.1	11.85
V	ME-MS41	ppm	33	235	214	189	169	213
W	ME-MS41	ppm	0.39	1.18	0.96	1.03	1.26	1.15
Y	ME-MS41	ppm	17.15	18.05	15.7	18.65	18.5	21.3
Zn	ME-MS41	ppm	67	864	162	357	869	408
Zr	ME-MS41	ppm	20.5	15.4	18.3	12.8	21	13
Au	PGM-ICP23	ppm	0.004	0.004	0.002	0.061	0.014	0.003
Pt	PGM-ICP23	ppm	<0.005	0.007	<0.005	0.011	0.009	0.006
Pd	PGM-ICP23	ppm	0.001	0.021	0.02	0.009	0.043	0.017
Li	ME-4ACD81	ppm	40	40	40	40	40	40
Tl	ME-MS42	ppm	0.1	1.43	1.12	0.75	0.89	0.92
Ge	ME-MS81	ppm	<5	<5	<5	<5	<5	<5
In	ME-MS42	ppm	0.011	0.084	0.014	0.037	0.089	0.042
Re	ME-MS42	ppm	0.001	0.186	0.158	0.169	0.193	0.163

Table A3. Samples TOB180255A, TOB180258A, TOB180260A, TOB190156A and TOB190157A.

Sample ID			TOB180255A	TOB180258A	TOB180260A	TOB190156A	TOB190157A
Easting (SWEREF99TM)			541694	541667	541621	537115	536637
Northing (SWEREF99TM)			6662171	6662147	6662004	6661588	6661965
Sample type			Waste rock	Waste rock	Outcrop	Outcrop	Outcrop
Location			Troengsgruvan	Ångmansgruvan	Gilltjärnsbergsgruvan	Sörskogen near Styggberget	Sörskogen near Styggberget
C	C-IR07	%	0.18	20.3	18.2	0.06	0.07
S	S-IR08	%	1.33	1.33	0.17	0.06	0.38
SiO2	ME-ICP06	%	47.8	53.2	58.9	53.2	73
Al2O3	ME-ICP06	%	17	9.39	7.62	14	13.05
Fe2O3	ME-ICP06	%	10.15	6.49	7.44	11.2	3.41
CaO	ME-ICP06	%	11.2	0.32	0.1	7.37	0.8
MgO	ME-ICP06	%	7.7	0.61	0.82	8.22	0.77
Na2O	ME-ICP06	%	0.42	0.33	0.01	0.31	1.31
K2O	ME-ICP06	%	2.18	2.75	2.01	2.69	4.55
Cr2O3	ME-ICP06	%	0.026	0.02	0.016	0.07	0.009
TiO2	ME-ICP06	%	0.66	0.45	0.3	1.02	0.42
MnO	ME-ICP06	%	0.18	0.01	0.02	0.18	0.02
P2O5	ME-ICP06	%	0.08	0.25	0.17	0.15	0.08
SrO	ME-ICP06	%	0.02	<0.01	<0.01	0.02	0.01
BaO	ME-ICP06	%	0.01	0.04	0.02	0.03	0.09
Ba	ME-MS81	ppm	120.5	325	211	255	705
Ce	ME-MS81	ppm	15.7	37.6	27	24.1	57.2
Cr	ME-MS81	ppm	150	110	90	430	50
Cs	ME-MS81	ppm	4.63	3.01	1.71	8.17	1.82
Dy	ME-MS81	ppm	2.55	4.29	2.44	3.11	2.61
Er	ME-MS81	ppm	2.01	2.66	1.85	1.97	1.65
Eu	ME-MS81	ppm	0.85	0.83	0.62	0.88	0.84
Ga	ME-MS81	ppm	19	18.4	14.2	17.7	14.5
Gd	ME-MS81	ppm	2.92	4.74	2.17	3.23	3.41
Hf	ME-MS81	ppm	1	2.7	2.2	1.8	4.4
Ho	ME-MS81	ppm	0.53	0.81	0.5	0.58	0.46
La	ME-MS81	ppm	7.2	20.7	14.9	11.1	28.8
Lu	ME-MS81	ppm	0.27	0.58	0.33	0.28	0.25
Nb	ME-MS81	ppm	3.3	12.9	6.6	5.5	8.8
Nd	ME-MS81	ppm	9.9	16.8	14.3	14.3	26.3
Pr	ME-MS81	ppm	2.03	4.9	3.7	3.39	7.1
Rb	ME-MS81	ppm	147	101.5	84.5	150	153.5
Sm	ME-MS81	ppm	2.35	4.06	3.25	3.33	4.14
Sn	ME-MS81	ppm	3	4	3	3	2
Sr	ME-MS81	ppm	288	29.5	15	249	151.5
Ta	ME-MS81	ppm	0.1	1.1	0.4	0.4	0.9
Tb	ME-MS81	ppm	0.45	0.69	0.29	0.54	0.51
Th	ME-MS81	ppm	1.1	8.54	6.62	2.89	9.94
Tm	ME-MS81	ppm	0.24	0.38	0.15	0.25	0.21
U	ME-MS81	ppm	0.46	8.44	9.62	1.24	3.63
V	ME-MS81	ppm	253	812	611	286	51
W	ME-MS81	ppm	2	11	9	2	2
Y	ME-MS81	ppm	15.3	25.6	14.7	16.4	13.4
Yb	ME-MS81	ppm	1.76	2.69	2.26	1.64	1.48
Zr	ME-MS81	ppm	34	113	77	71	168
As	ME-MS42	ppm	0.7	3.7	13.3	12.8	1.1
Bi	ME-MS42	ppm	0.33	2.29	1.4	0.11	0.31
Hg	ME-MS42	ppm	0.011	0.006	<0.005	<0.005	<0.005
Sb	ME-MS42	ppm	0.25	0.11	<0.05	0.09	0.09
Se	ME-MS42	ppm	1.7	15.5	5.6	<0.2	0.6
Te	ME-MS42	ppm	0.07	0.41	0.22	0.02	0.01
LOI	OA-GRA05	%	3.51	25.8	22.3	2.59	2.97
Total	TOT-ICP06	%	100.94	99.66	99.73	101.05	100.49
Ag	ME-4ACD81	ppm	<0.5	0.6	0.5	<0.5	<0.5
Cd	ME-4ACD81	ppm	0.8	<0.5	<0.5	0.7	<0.5
Co	ME-4ACD81	ppm	49	1	2	31	2
Cu	ME-4ACD81	ppm	106	37	118	15	35
Mo	ME-4ACD81	ppm	2	77	49	2	2
Ni	ME-4ACD81	ppm	30	53	48	22	7
Pb	ME-4ACD81	ppm	8	13	4	4	22
Sc	ME-4ACD81	ppm	38	14	9	35	7

Table A3. Continuation.

Sample ID			TOB180255A	TOB180258A	TOB180260A	TOB190156A	TOB190157A
Easting (SWEREF99TM)			541694	541667	541621	537115	536637
Northing (SWEREF99TM)			6662171	6662147	6662004	6661588	6661965
Sample type			Waste rock	Waste rock	Outcrop	Outcrop	Outcrop
Location			Troengsgruvan	Ångmansgruvan	Gilltjärnsbergsgruvan	Sörskogen near Styggberget	Sörskogen near Styggberget
Zn	ME-4ACD81	ppm	115	38	143	128	31
Ag	ME-MS41	ppm	0.29	0.73	0.59	0.02	0.11
Al	ME-MS41	%	2.4	0.52	1.32	3.25	0.88
As	ME-MS41	ppm	0.6	3.6	12.7	12.9	1.1
Au	ME-MS41	ppm	<0.02	<0.02	<0.02	<0.02	<0.02
B	ME-MS41	ppm	10	<10	<10	<10	<10
Ba	ME-MS41	ppm	20	10	10	160	20
Be	ME-MS41	ppm	0.22	0.62	0.53	0.31	0.28
Bi	ME-MS41	ppm	0.36	2.36	1.45	0.1	0.29
Ca	ME-MS41	%	2.47	0.23	0.07	1.59	0.36
Cd	ME-MS41	ppm	0.1	0.01	0.27	0.05	0.02
Ce	ME-MS41	ppm	11.15	33.1	23.6	22	47.1
Co	ME-MS41	ppm	36.7	1.6	2.5	19	3.7
Cr	ME-MS41	ppm	28	28	39	230	28
Cs	ME-MS41	ppm	1.82	0.93	0.56	6.79	0.37
Cu	ME-MS41	ppm	98	35.1	114	15	37.8
Fe	ME-MS41	%	2.83	4.1	4.97	4.02	2.4
Ga	ME-MS41	ppm	3.8	3.94	5.31	8.99	4.67
Ge	ME-MS41	ppm	0.1	0.17	0.18	0.12	<0.05
Hf	ME-MS41	ppm	0.04	0.37	0.21	0.1	0.25
Hg	ME-MS41	ppm	0.01	0.01	0.01	<0.01	<0.01
In	ME-MS41	ppm	0.013	0.013	0.036	0.025	0.012
K	ME-MS41	%	0.18	0.1	0.07	1.21	0.14
La	ME-MS41	ppm	5.8	17.6	13.1	11.2	24
Li	ME-MS41	ppm	26.5	6.1	23.9	47.2	17.1
Mg	ME-MS41	%	0.65	0.21	0.37	2.17	0.4
Mn	ME-MS41	ppm	134	51	118	300	143
Mo	ME-MS41	ppm	0.97	72.6	47.1	0.81	1.29
Na	ME-MS41	%	0.03	0.01	0.01	0.04	0.01
Nb	ME-MS41	ppm	0.12	0.05	<0.05	0.26	0.82
Ni	ME-MS41	ppm	22.1	50.7	44.8	14.8	7.4
P	ME-MS41	ppm	510	1060	670	620	330
Pb	ME-MS41	ppm	4.7	10.8	6.5	4.6	10.3
Rb	ME-MS41	ppm	13.7	8.5	5.6	73.1	7.5
Re	ME-MS41	ppm	<0.001	0.181	0.086	0.001	0.001
S	ME-MS41	%	1.31	1.35	0.18	0.04	0.44
Sb	ME-MS41	ppm	0.29	0.14	0.05	0.09	0.09
Sc	ME-MS41	ppm	2.1	0.8	1.2	12.9	2.1
Se	ME-MS41	ppm	1.7	15.9	5.6	<0.2	0.6
Sn	ME-MS41	ppm	0.3	0.5	0.6	0.9	0.6
Sr	ME-MS41	ppm	40.5	3.7	2.7	42	6.7
Ta	ME-MS41	ppm	<0.01	<0.01	<0.01	<0.01	0.01
Te	ME-MS41	ppm	0.05	0.37	0.19	0.02	0.01
Th	ME-MS41	ppm	1	6.8	6.1	2.8	10.3
Ti	ME-MS41	%	0.073	0.013	<0.005	0.309	0.146
Tl	ME-MS41	ppm	0.1	0.33	0.07	0.52	0.09
U	ME-MS41	ppm	0.38	6.95	9.11	0.8	3.3
V	ME-MS41	ppm	37	142	203	139	22
W	ME-MS41	ppm	1.04	1.1	0.93	0.22	0.26
Y	ME-MS41	ppm	1.82	14.45	11.7	4.91	8.08
Zn	ME-MS41	ppm	31	31	139	75	28
Zr	ME-MS41	ppm	1.6	14.7	7.9	4.8	7.5
Au	PGM-ICP23	ppm	0.006	0.006	0.006	<0.001	0.001
Pt	PGM-ICP23	ppm	<0.005	0.023	0.013	<0.005	<0.005
Pd	PGM-ICP23	ppm	0.002	0.012	0.01	0.001	0.002
Li	ME-4ACD81	ppm	50	20	30	60	20
Tl	ME-MS42	ppm	0.1	0.33	0.07	0.52	0.09
Ge	ME-MS81	ppm	<5	<5	<5	<5	<5
In	ME-MS42	ppm	0.013	0.013	0.036	0.025	0.012
Re	ME-MS42	ppm	<0.001	0.176	0.084	0.001	0.001

APPENDIX B. PETROPHYSICAL ANALYSIS RESULTS

Table B1. Results from petrophysical analyses of bedrock samples from mine waste and outcrop by the Giltjärn and Skrammelfall mines and surrounding area northwest of Norberg.

Sample ID	Easting (SWEREF99TM)	Northing (SWEREF99TM)	Bedrock	Location	Geophysical Profile	Density (kg/m ³)	Magnetic Susceptibility (10 ⁻⁶ SI)	Natural Remanent Magnetisation (10 ⁻³ A/m)	Q-value
TOB190119A	542806	6663121	Greywacke	<i>Blyertsgruvan</i>	1, 2, 3	2804	647	41	1.6
TOB190119B	542806	6663121	Greywacke	<i>Blyertsgruvan</i>	1, 2, 3	2546	122	39	8.0
TOB190119C	542806	6663121	Greywacke	<i>Blyertsgruvan</i>	1, 2, 3	2757	297	28	2.3
TOB190120A	542710	6663185	Greywacke	Skrammelfall mines	1, 2, 3	2688	83	48	14.6
TOB190121A	542660	6663285	Greywacke	Skrammelfall mines	1, 2, 3	2749	388	94	6.0
TOB190122A	542678	6663322	Greywacke	<i>Gamla Skrammelfallsgruvan 1</i>	1, 2, 3	2685	10335	5788	14.0
TOB190122B	542678	6663322	Greywacke	<i>Gamla Skrammelfallsgruvan 1</i>	1, 2, 3	2614	200	59	7.4
TOB190122C	542678	6663322	Greywacke	<i>Gamla Skrammelfallsgruvan 1</i>	1, 2, 3	2637	1699	1123	16.5
TOB190122D	542678	6663322	Greywacke	<i>Gamla Skrammelfallsgruvan 1</i>	1, 2, 3	2691	16972	6304	9.3
TOB190123A	542610	6663335	Greywacke	Skrammelfall mines	1, 2, 3	2698	256	121	11.8
TOB190124A	542561	6663422	Greywacke	Skrammelfall mines	1, 2, 3	2689	289	21	1.9
TOB190125A	545918	6667065	Tonalite		4	2763	412	19	1.2
TOB190129A	545188	6667252	Greywacke		4	2732	308	20	1.6
TOB190130A	545545	6667559	Greywacke	<i>Ekorrsvedsgruvan</i>		2823	304	65	5.3
TOB190130B	545545	6667559	Greywacke	<i>Ekorrsvedsgruvan</i>		2685	3507	9059	64.6
TOB190131A	546063	6668415	Greywacke		5	2723	300	20	1.7
TOB190132A	545879	6668383	Greywacke		5	2721	362	37	2.6
TOB190133A	545597	6668062	Greywacke		5	2732	335	18	1.4
TOB190134A	545323	6667997	Greywacke		5	2764	273	32	2.9
TOB190135A	545062	6668088	Greywacke		6	2714	244	41	4.2
TOB190136A	545019	6668178	Greywacke		6	2734	286	23	2.0
TOB190137A	544798	6668239	Greywacke		6	2721	349	56	4.0
TOB190139A	544744	6668796	Greywacke		6	2904	567	30	1.3
TOB190140A	545566	6668240	Greywacke		5	2685	181	8	1.1
TOB190141A	542017	6661697	Greywacke		7	2738	262	12	1.2
TOB190142A	542007	6661782	Greywacke		7	2771	331	16	1.2
TOB190143A	541928	6661816	Rhyolite		7	2670	531	2793	131.4
TOB190144A	541744	6661998	Greywacke	<i>Troengsgruvan</i>	7	2734	279	25	2.2
TOB190145A	541638	6662061	Greywacke	<i>Troengsgruvan</i>	7	2709	207	20	2.4
TOB190146A	541635	6662075	Greywacke	<i>Troengsgruvan</i>	7	2653	123	15	3.0
TOB190147A	541539	6662151	Greywacke	<i>Troengsgruvan</i>	7	2742	383	318	20.8
TOB190148A	541473	6662199	Greywacke		7	2735	820	148	4.5

Table B1. Continuation.

Sample ID	Easting (SWEREF99TM)	Northing (SWEREF99TM)	Bedrock	Location	Geophysical Profile	Density (kg/m ³)	Magnetic Susceptibility (10 ⁻⁶ SI)	Natural Remanent Magnetisation (10 ⁻³ A/m)	Q-value
TOB190149A	541358	6662312	Greywacke		7	2703	217	24	2.7
TOB190150A	542353	6662446	Greywacke		8	2718	256	29	2.8
TOB190151A	542312	6662459	Greywacke		8	2727	252	12	1.2
TOB190152A	542236	6662468	Greywacke		8	2610	105	19	4.5
TOB190153A	542097	6662547	Greywacke		8	2704	213	63	7.4
TOB190154A	541856	6662605	Greywacke		8	2723	275	15	1.4
TOB190155A	541571	6662846	Granodiorite		8	2680	252	54	5.4
TOB190156A	537115	6661588	Amphibolite		9	3009	765	61	2.0
TOB190157A	536637	6661965	Greywacke		9	2666	150	24	4.0
TOB190158A	536062	6662656	Granodiorite		9	2841	644	10	0.4